RICE UNIVERSITY

THE OMEGA PHASE IN TITANIUM-VANADIUM ALLOYS

by

John E. Gragg, Jr.

A THESIS SUBMITTED
IN PARTIAL FULFILLMENT OF THE
REQUIREMENTS FOR THE DEGREE OF

MASTER OF SCIENCE

Thesis Director's Signature:

Original Signed
By Franz R. Brotzen

Houston, Texas
May, 1964

ABSTRACT

The precipitation of the omega phase in quenched titanium-vanadium alloys of 15% to 25% vanadium was investigated by x-ray analysis and resistivity measurements.

The omega phase precipitation was found to be controlled by an enhanced diffusion mechanism which was closely linked to a pre-precipitation process occurring in these alloys.

This pre-precipitation process is believed to be the cause of the negative temperature coefficient of resistance observed in these alloys below $0^{o}C$.

Contrary to the results of previous investigations, no martensitic transformation of the beta phase to the omega phase was observed at low temperatures.

TABLE OF CONTENTS

INTRODUCTION

In the pure metal, titanium undergoes an allotropic transformation at 883°C from a high temperature, body-centered cubic structure to a low temperature, hexagonal close-packed structure. These two phases are called the beta and alpha structures respectively.

There are many substitutional alloying elements, however, which in sufficient quantities can stabilize the β-phase at temperatures far below 883°C. An example of one of these stabilizing elements is the metal vanadium. As observed by Duwez et al.[1][2], the continuous addition of vanadium to titanium lowers the M_s temperature to approximately 13% vanadium and 300°C, where the M_s point van[illegible]. It seems doubtful that the M_s point would vanish, although it probably does go below room temperature for more than 15% vanadium. Thus, it seems that for sufficient quantities of these stabilizing elements, it should be possible to produce by rapid quenching an alloy consisting only of a "metastable" β-structure at room temperature.

Brotzen et al.[3] have observed that for titanium-base alloys containing more than 12.5% vanadium, rapid quenching of the alloys caused the retention of large amounts of the metastable β-phase. Frost et al.[4][5] have observed similar β-retention in titanium-base alloys of 7.54% chromium, 7.73% manganese, 10% molybdenum, and 4% and 5% iron.

Associated with this metastable β-structure are some pronounced changes in the physical properties of the alloys. One of the most important of these properties is a drastic increase in hardness of these alloys when aged at low temperatures (less than 450°C). This is in contrast with the supersaturated α'-phase which can be formed by quenching

in alloys of low concentrations (less than 15% for vanadium) which remains relatively soft when aged.

Frost was among the first to investigate this hardening effect in titanium-base alloys of chromium and manganese[4][5]. He was able to establish the presence of a transition phase of unidentified lattice structure in both alloys which formed during ageing which he designated omega. It was this ω-phase which Frost felt was responsible for the age hardening in these metastable alloys. Brotzen, in investigating the decomposition of the metastable β-phase in titanium-vanadium alloys[3], established the presence of the ω-phase in these alloys which was formed as a coherent structure with the parent β-phase during the course of low temperature ageing. The process of the β-decomposition in titanium-vanadium alloys was found to be,

$$\beta \longrightarrow \beta + \omega \longrightarrow \omega + \alpha \longrightarrow \alpha$$

where the second and third steps were bypassed at high reaction temperatures.

The structure of the ω-phase in a Ti-16% alloy has been investigated by Silcock et al.[6] and determined to be hexagonal with $a = 4.60\text{Å}$ and $c = 2.82\text{Å}$. The atomic positions were found to be (0,0,0) and $\pm$ (1/3, 2/3, 1/2) while the orientation relationship was $[0001]_\omega \parallel [111]_\beta$ and $(11\bar{2}0)_\omega \parallel (110)_\beta$ with the plane of coherence being $(11\bar{2}0)_\omega$. Bagaryatskii et al.[7] independently investigated the ω-structure in titanium-chromium alloys and proposed a structure similar to Silcock's, the only difference being the atomic positions which were found to be (0,0,0) and $\pm$ (1/3, 2/3, 0.48)[8]. Silcock, in a later work[9], found that, at least in the titanium-vanadium alloys, z was very close to 1/2,

being $z = 0.495 \pm 0.005$. Both of these investigators were working with quenched alloys which had been aged at 400-450°C.

This ω-structure has been observed in titanium-base alloys of chromium, manganese, molybdenum, iron, vanadium, niobium, and even uranium[8]. Work with the heavier alloying elements has indicated that this phase has no ordered structure, since no superlattice lines have ever been observed. In addition, the ω-structure has been observed in several zirconium-base alloys.

Hatt and Roberts[10] have investigated the ω-phase in both quenched and annealed zirconium-niobium alloys and have found a hexagonal structure in both the quenched and annealed states. The two structures differ, however, in their respective c/a ratios and in their atomic positions. In the quenched state, the ω-structure was found to have c/a = 0.622 with the atomic positions (0,0,0) and $\pm$ (1/3, 2/3, 0.58), while the annealed structure was found to have c/a = 0.616 and atomic positions (0,0,0) and $\pm$ (1/2, 2/3, 1/2). The former structure is in reasonable agreement with the results of Bagaryatskii while the latter is in agreement with the results of Silcock. However, since nothing is known about the ageing treatment used by Bagaryatskii it is not possible to reach any immediate conclusions concerning the general nature of the ω-structure.

It has been observed in general that, particularly in the lower percentage alloys, the ω-phase was present after quenching. Bagaryatskii[7] has observed that for sufficiently low concentrations of the alloying element it was not possible to suppress the formation of the ω-phase even by drastic quenching. Thus, it appears that it may be possible

to form the ω-phase athermally as well as by annealing. If such a martensitic transformation of β to ω were to occur, however, from the usual shear definition of a martensitic transformation one would expect to be able to observe the ω-phase by the surface relief produced by such a transformation. No such relief has ever been observed in alloys known to contain large amounts of transformed ω-phase. For this reason, Bagaryatskii has referred to the β to ω transformation as "a singular kind of martensitic transformation"[7].

One possible explanation for this lack of surface relief lies in the mechanism of the β to ω transformation. This mechanism, proposed by both Silcock and Bagaryatskii, consists of sets of alternating shears of magnitude 1/6 $[111]_\beta$ in the $[111]_\beta$ direction on the $(110)_\beta$ planes. This can be seen in Fig. 2. Such a transformation might well produce no optically visible surface relief.

One of the most unusual effects observed in these metastable titanium-base alloys is the negative temperature coefficient of resistance observed by Brotzen[3] in quenched alloys of 15-20% vanadium below 0°C. Hehemann[11] has recently found evidence of a low temperature athermal transformation of the metastable β-phase to the ω-structure in zirconium-niobium alloys below 0°C which he feels is responsible for this unusual resistivity effect. However, no direct correlation of this low temperature transformation and the resistivity effect has yet been made.

Since so little is known of the detailed behavior of the formation of the ω-phase from the metastable β-phase, both at high and low temperatures, it is the aim of this investigation to provide some insight into how the variables of time, temperature, and composition affect the properties of the β to ω transformation and the nature of the alloys.

MATERIALS AND PROCEDURES

A series of titanium-vanadium alloys ranging from 15% to 25% nominal vanadium weight composition was chosen for this particular investigation. They were prepared by Reactive Metals, Inc. from iodide-refined titanium and high purity electrolytic vanadium. An assay of these alloys provided by the manufacturer is given in Table 1.

A second series of titanium-vanadium alloys was obtained from Union Carbide Company and was used as a check against the first series in several cases. These alloys, however, were found to be of highly non-uniform composition and were not used in any of the primary investigations.

Both groups of alloys were received as circular bar stock. The series from Reactive Metals had been extruded into 3/8" diameter bar stock, while the Union Carbide alloys had been rolled into 3/8" diameter bar stock from cast round ingots. Both series of alloys exhibited a certain degree of preferred orientation due to the extruding and rolling operations.

Two different types of specimens were prepared from the alloys for x-ray and resistivity studies. The x-ray specimens were prepared as round buttons, 0.350" in diameter and 0.050" thick, with a mounting stub 0.150" long and 0.150" in diameter protruding from the back. The top surface of the specimen was polished on successively finer grit paper down to 600 grit and finally polished on an abrasive wheel with 0.3 micron Alumina grit. The specimen was then thoroughly cleaned and stored for later heat treatment.

The resistivity specimens were prepared as square bars 0.100" across in the central section approximately 2.250" long. The ends of

the bar were flared out to 0.250" wide and 0.375" long with holes drilled in this section for mounting in the measuring circuit. Both the x-ray and the resistivity specimens are shown in Figure 6.

The heat treatment of the specimens presented some particular problems due to the high solubility of hydrogen, nitrogen, and oxygen in titanium and its alloys and the necessity of quenching the specimens very rapidly from high temperatures (greater than 900°C). To meet these requirements, a high vacuum heat treating furnace was constructed which allowed the specimens to be quenched while still in the heating chamber. The heart of this system was a Vycor test tube mounted vertically in the load coil of a 10 kilowatt induction furnace. The top of the test tube was sealed with a rubber stopper with an inlet/outlet tube in it. This inlet/outlet tube could be opened to either a high vacuum pumping system or to an ice water quench bath.

The specimen to be heat treated was hung from a 0.001" tungsten wire inside the Vycor tube and the load coil of the induction furnace. The water in the quench bath was then drawn up to the down-stream side of the inlet valve, the system sealed, and then evacuated to less than 5×10^{-5} mm Hg. The specimen was then raised to a homogenizing temperature of approximately 975°C and held at this temperature for 20 to 60 minutes, depending on the composition of the alloy being used. At all times during the heat treatment, a vacuum of less than 5×10^{-5} mm. Hg was maintained to prevent contamination of the alloy by soluble gases.

At the end of the homogenizing period, the vacuum line was sealed off, the load coil shut off, and the inlet valve to the quench bath opened, allowing the quench water to flow directly into the Vycor test

tube. It was found that, at least with the smaller x-ray specimens, a very rapid quench could be obtained, resulting in 100% retained beta phase in even the 15% vanadium specimens with very little oxidation. It was determined that most of the oxidation that was present occurred on the quench and was mostly due to dissolved gases in the quench water. The larger resistivity specimens were found to be harder to quench due to the limited amount of quenching medium which could be admitted to the chamber and at times had to be heat treated again.

After heat treatment of the specimens, the light oxide layer which did form on the surface of the specimen was removed by electropolishing in a mixture of glycerin, nitric acid, and hydrofluoric acid in a 4:1:1 volume ratio mixture respectively. The glycerin base electrolyte was used to again prevent contamination of the alloys by the hydrogen and nitrogen ions which would have been present in a medium such as water which causes a strong degree of ionization, while the electropolishing was necessary because of the possibility of inducing a premature phase transformation in the quenched alloys due to the heat generated by mechanical polishing.

Two different annealing baths were used for the subsequent low temperature annealing work. At temperatures below 200°C, a constant temperature oil bath was used, while the work done at 400°C and above was performed in a molten lead bath. The specimens were again electropolished after each annealing period. In all of the annealing investigations, the specimens were quenched in ice water at the end of the annealing period. After the x-ray investigation, the specimens were returned to the annealing bath and the annealing procedure repeated to extend

the total annealing time.

Since it was desired to study these alloys at subzero temperatures during the course of the x-ray phase of this investigation, an x-ray cryogenic diffractometer mount was developed for use with a General Electric XRD 5 X-Ray Diffractometer. This mount consisted of a copper cooling block mounted on a base and pedestal so that the face of the block was normal to the base of the x-ray goniometer and to the plane bisecting the incident and reflected x-ray beam.

Provisions were made so that the x-ray specimen could be placed on the face of this mount in thermal contact with the cooling block. The face of the cooling block and the specimen could then be covered with a Saran* window which prevented moisture from condensing onto the specimen and block and forming ice during the course of a low temperature run. The block itself was cooled by admitting liquid nitrogen into a chamber on the back side of the block which contained a set of cooling fins parallel to and approximately 1/2" behind the face of the cooling block.

Since it was found that the temperature of the specimen was not in phase with the temperature of the cooling block, the temperature controlling signal was taken from a copper-constantan thermocouple clamped to the surface of the specimen. This signal was fed into a Leeds and Northrup Speedomax 60H Proportional On-Off Controller which in turn activated a normally closed solenoid valve in the nitrogen line leading to the cooling chamber of the x-ray cryostat. With this apparatus used in this configuration, temperatures as low as -70°C could be obtained and controlled to within $\pm$ 0.5°C. For studies at liquid

*Registered Trademark, Dow Chemical Company

nitrogen temperatures, the Saran window was removed and the specimen was cooled by a direct and continuous flow of gaseous nitrogen.

Figures 3 and 4 show this x-ray cryostat in perspective and in cross-section. The previously mentioned cooling fins are shown in Figure 4 in cross-section and consist of a set of concentric circular fins of decreasing height outward along the radius of the circular cooling block. Not shown in this figure is a nylon plug which fitted into the back of the cooling chamber and formed a diverging nozzle for the entering stream of nitrogen coolant, directing the stream onto the cooling fins.

One of the reasons for the limit on the lowest temperature attainable with this apparatus was the high heat flow into the cooling block through the base and pedestal assembly. However, such a heavy mounting system for the cooling block was found to be necessary in order to prevent the face of the block from moving out of alignment with the goniometer head as it was cooled. Although this movement was small (on the order of 0.010"), it was found to produce pronounced changes in the relative intensities of the individual diffraction peaks, and made any analysis of the phase composition of the alloy impossible. Later studies indicated that most of the movement of the mount was produced by the constraint of the coolant transfer hose on the cooling block. The heavier and more massive pedestal and base assembly was the only positive solution found to this problem.

The resistivity phase of this investigation was performed on two different pieces of equipment. The first apparatus used was a four terminal a.c. resistance bridge with the balance point being detected

by the oscilloscope trace of the output of a differential amplifier. This apparatus is shown schematically in Figure 5. The second piece of equipment to be used in this part of the investigation was a standard Wheatstone bridge circuit with a Leeds and Northrup Micro-ohm Slidewire used as the standard resistance scale. With this particular piece of equipment, it was possible to detect the balance point to within $\pm$ 0.5μohms. The resistivity specimen itself was immersed in an isopentane cooling bath which was maintained at a constant temperature by the same temperature controlling circuit that was used for the x-ray cryostat. The temperature of this bath could be controlled to within $\pm$ 0.25^{o}C down to -140^{o}C.

RESULTS

As was mentioned previously in this paper, the theory has been advanced by several investigators that it is possible to form the ω-phase from the metastable quenched β-phase by an athermal shear mechanism. Moreover, it has been proposed that the negative temperature coefficient of resistivity observed in these metastable β-structures below 0°C is due to the formation of the ω-phase by such an athermal transformation. For this reason, the initial phase of this investigation consisted of a series of x-ray diffraction studies of quenched Ti-V alloys at temperatures down to -196°C.

The specimens were analyzed for volume percent phase composition using the method of integrated intensities of Cohen and Averbach[12]. This method is based on the relationship between the integrated intensity of a diffraction peak and the various angular and structural factors associated with the peak. The derivation of the method is given in Appendix I for a two phase system.

The results found in Appendix I are:

$$V_\beta = 1/(1 + \gamma)$$

$$V_\omega = \gamma/(1 + \gamma)$$

where,

V_ω, V_β = Volume-% phase compositions

$\gamma = K(\omega,\beta)\ A(\theta_\omega)\ S_\omega / A(\theta_\beta) S_\beta$

$K(\omega,\beta)$ = A calculated constant

$A(\theta_x)$ = Angular adsorption factor at angle $2\theta_x$

S_x = Integrated intensity of "x"-phase peak at angle $2\theta_x$.

Thus, with this method of analysis, it is possible to compute the volume-% phase composition from the measured integrated intensities of the diffraction peaks and the knowledge of the structure of the phases associated with the peaks.

The one parameter in Eqn. (1) of Appendix I which cannot be known directly from intensity measurements of single lines is the angular adsorption factor, $A(\theta)$. However, for a flat specimen such as was used in this investigation, $A(\theta)$ is a constant for θ equal to the glancing angle. In addition, the majority of the work done in this investigation involved diffraction peaks from the β- and ω-phases which were in close angular proximity to each other, minimizing any changes in $A(\theta)$ due to misalignment of the diffraction mount.

The low-temperature investigation was carried out using nominal alloy compositions of 15%, 20% and 25% vanadium. Immediately after heat treatment, the quenched specimen was electropolished and placed in the x-ray cryostat. In the 15% alloys, only minute traces of the ω-phase could be detected after quenching, and then only by scaling the output of the detector on a digital scaler about the calculated positions of the ω-peaks, while the 20% and 25% vanadium alloys appeared to be 100% β-phase. Moreover, in the majority of the specimens investigated, only the most intense ω-peaks could be detected by the scaling technique.

One of the problems found in comparing the intensities of the coherent ω- and β-peaks was the coincidence of many of the individual peaks. In the angular range investigated, as can be seen in Table 2, there was only one β-peak which did not coincide with a coherent ω-peak. However, there were ω-peaks which could be detected by scaling which

did not coincide with any of the β-peaks. These were the peaks which were used for the low temperature studies.

In brief, the result of this phase of the investigation was negative, i.e.- no low temperature phase transformation from β to ω could be detected by any increase in the ω-peak intensities or any decrease in the β-peak intensities at temperatures down to -196°C in any of the alloys. This is in strong contrast with the work of Hehemann[11] who observed a four-fold increase of the ω-peak intensities in Zr-Nb quenched alloys at -196°C.

The second phase of this investigation consisted of a study of the kinetics of the precipitation of the ω-phase from the metastable β-phase as a function of time, temperature, and composition. The object of this particular investigation was to obtain some insight into the nature of the quenched β-structure from the behavior of the ω-precipitation kinetics.

The most striking effect found in the ω-precipitation was the rapidity with which the ω-phase was formed. In the Ti-20%V quenched alloy, over 60% of the volume was transformed to the ω-phase after 100 secs. at 425°C. The initial period of this precipitation was even more rapid in the quenched Ti-15%V alloy, although the process began to slow down to a rate below that of the Ti-20%V alloy after approximately 30 secs. at 425°C. In the Ti-22.5%V alloy, the process of precipitation was found to be slower than in the Ti-20%V alloy and required higher reaction temperatures to initiate. However, the process was still quite rapid and produced over 25 volume-% of ω-phase after 100 secs at 500°C (Figure 7).

The volume-% of ω-phase for this annealing work was computed from the relative intensities of the $(110)_\beta$ peaks which occurred at $2\theta \doteq 39.8^\circ$ for Cu K α radiation and the $(11\bar{2}0)_\omega$ and $(10\bar{1}1)_\omega$ peaks which were superimposed on each other just below 39.8°. An example of these calculations is given for a Ti-20%V alloy annealed at 425°C in Table 3.

As can be seen in Table 2, however, for the perfectly coherent ω-phase the $(11\bar{2}0)_\omega$ and $(10\bar{1}1)_\omega$ peaks occur at the same 2θ angle as the $(110)_\beta$ peak. Thus, it was possible to distinguish these two peaks only because of a rapid shift of the ω-peaks to lower 2θ angles as the precipitation progressed. In the Ti-20%V alloy, shifts of greater than 0.5° were observed for the ω-peaks. No corresponding shift to higher 2θ angles was observed for the βpeaks, however, until long after the precipitation process had ceased and an equilibrium phase composition had been established.

During the early stage of the ω-precipitation (less than 60 secs.), the ω-peaks were quite broad and the two peaks below 39.8° could not be resolved. Particle size estimates of the ω-precipitate from the half-width of this combined peak gave minimum dimensions of 200-400Å. Only in the later stages of precipitation and after phase equilibrium was established did the two peaks sharpen and become capable of being resolved.

Although the precipitation of the ω-phase from the metastable β-phase occurred so rapidly, the reversion of ω to β occurred quite slowly in comparison.

In a Ti-20%V specimen which had transformed 80 volume-% to the ω-phase during low temperature annealing, it was found that over 60 mins.

at 950°C was required to transform the ω-phase back to the β-phase. This process was observed by heating the specimen in the high-vacuum heat-treating furnace for the desired annealing time and then quenching the specimen in ice water. The phase composition was then determined by x-ray analysis and the specimen returned to the furnace for further annealing. The reversion process appeared to follow the same path as the precipitation process, with the ω-peaks shifting back toward the positions of the perfectly coherent ω-phase as the ω-phase reverted to β-phase.

These results seem to indicate a relationship between the lattice parameters of the ω-phase and the volume-% of the ω-phase present, although this relationship also appears to be a function of composition, annealing temperature, severity of quenching, and many other "structural" factors.

In all of the alloys, the initial stage of ω-precipitation was found to be proportional to $t_a^{\frac{1}{2}}$, where t_a = the annealing time. This is the normal relationship for a one dimensional diffusion controlled process. Moreover, the ω-phase lattice parameters in all of the alloys during this initial stage of precipitation were found to be proportional to the annealing time (Figures 9 and 12).

This rapid rate of ω-formation has been postulated by many of the investigators who have worked with the ω-phase in these metastable β-alloys. Krisement[13], through calorimetric studies of the decomposition of the metastable β-phase in Ti-V alloys, concluded that the rate of formation of the ω-phase was much too rapid to be explained by normal bulk diffusion. Thus, the question remained that if some form of "enhanced"

diffusion was occurring during the ω-precipitation, what was the mechanism responsible for it?

It has been reported by Harmon and Troiano[14] that prolonged ageing of quenched Ti-V alloys at 250°C produced a splitting of the β-peaks while forming no ω-phase. This process may well be associated with the mechanism which causes the rapid formation of the ω-phase at higher temperatures. For this reason, the next phase of the investigation consisted of a study of the effect of very low temperature annealing on later ω-precipitation at higher temperatures. This very low temperature annealing was performed in a constant temperature oil bath at 200°C.

In the Ti-15%V alloy, it was observed that the ω-phase was formed even at this very low annealing temperature, although at a much slower rate than at 425°C (Figure 8). In the Ti-20%V and Ti-22.5%V alloys, however, annealing for several hours at 200°C produced no ω-phase. For this reason, the very low temperature annealing in the alloys above 15% vanadium was referred to as stabilization by incubation rather than annealing.

The most striking effect observed as a result of stabilization was a drastic decrease in the rate of ω-formation on subsequent high temperature annealing. This effect was greatest in the Ti-20%V alloy, with a 40 min. stabilization at 200°C causing a 75% decrease in the volume-% ω-phase formed in 100 secs. at 425°C (Figure 10). The deviation of the precipitation following stabilization from the $t_a^{\frac{1}{2}}$ dependence of precipitation in the quenched Ti-20%V alloy is shown in Figure 11.

The effect of stabilization on subsequent precipitation was not so pronounced in the Ti-22.5%V alloy, with a 20 min. incubation at 200°C producing a 25% decrease in the volume-% ω-phase formed after 240 secs. at 500°C (Figure 13).

No x-ray data is shown for the Ti-25%V alloy, since the β-phase in this alloy was found to be stable with respect to ω-precipitation at reaction temperatures above 400°C for 10-20 mins. However, it was suspected that even though no rapid ω-precipitation was observable in this alloy, the same mechanism which was demonstrated by the effect of stabilization in the Ti-20%V and Ti-22.5%V alloys was also operative in this alloy.

In order to compare the mechanism activated by stabilization in the various alloys, the last phase of this investigation consisted of a study of the effect of stabilization on the electrical resistance and its temperature coefficient as a function of % vanadium.

As previously mentioned, the quenched β-structure demonstrated a negative temperature coefficient of resistance below 0°C. This temperature coefficient of resistance was found to be increasingly negative with increasing vanadium content of the alloys (Figure 14). The Ti-15%V alloy did not exhibit this behavior, however. One possible explanation of this is the dependence of this effect on the previous quench. It was observed that the more severe the quench, the more pronounced was the increase in resistance with decreasing temperature. Thus, the behavior of the 15% vanadium specimen may be due to a poor quench, although this effect was observed in two different Ti-15%V specimens.

The effect of stabilization produced some unusual results in the Ti-20%V and Ti-25%V alloys. The most drastic change in the behavior of the resistance at low temperatures was observed in the Ti-20%V alloy, where the temperature coefficient of resistance actually became more negative after 20 mins. stabilization at 200°C. Further stabilization raised the initial coefficient at 0°C, although the coefficient was still more negative than in the quenched alloy at -120°C (Figure 15).

Annealing at 400°C, which was known to form ω-phase, rapidly increased the temperature coefficient of resistance in the Ti-20%V alloy and the coefficient soon reached a normal positive behavior (Figure 16), In all of the alloys, quenched, annealed, and stabilized, the resistance behavior was found to be completely reversible with temperature and demonstrated no detectable temperature hysterisis (Figure 16).

The effect of stabilization on the Ti-25%V alloy was less pronounced than in the Ti-20%V alloy and served only to reduce the increase in resistance with decreasing temperature. However, it is important to note that stabilization at 200°C produced this change in resistance behavior in an alloy which was found to retain the metastable β-structure even at 400°C (Figure 17).

Another unusual and important behavior of these alloys during stabilization is the <u>increase</u> in resistance observed during increasing stabilizing time (Figure 18). This is in contrast with the resistance behavior of quenched Ti-V alloys during annealing at 450°C, which was observed by Brotzen et al.[3] to decrease with increasing annealing time (Figure 19).

Finally, Figures 20-22 show some general examples of the intensity behavior of the β-peaks and the ω-peaks during annealing for the different alloys investigated.

The results of these experiments may be summarized as follows:

(1) No low temperature athermal transformation of β to ω in titanium-base alloys of 15% to 25% vanadium could be observed by x-rays.

(2) The ω-phase precipitated from the metastable β-phase at a very rapid rate between 200°C and 500°C with the amount formed proportional to $t_a^{\frac{1}{2}}$ and accompanied by an increase in the ω-phase lattice parameter. No change in the β-phase lattice parameter was observed until long after the ω-precipitation had ceased. The change in the β-lattice parameter was accompanied by an increase in sharpness of the ω-phase peaks.

(3) The rate of initial ω-precipitation decreased with increasing vanadium content of the alloys.

(4) Stabilization of the metastable β-phase at 200°C produced no detectable precipitation in the alloys above 15% vanadium, yet significantly reduced the rate at which subsequent ω-precipitation did occur on high temperature annealing.

(5) The metastable β-phase in the alloys above 15% vanadium exhibited an increase in resistance with decreasing temperature.

(6) The temperature coefficient of resistance was found to be increasingly negative with increasing vanadium content of the alloys.

(7) Stabilization of the metastable β-phase at 200°C produced some pronounced changes in the low temperature resistance behavior of these alloys, even to making the temperature coefficient of resistance more negative. This is in contrast to the observed increase in the temperature coefficient of resistance on annealing at high temperatures.

(8) Stabilization of the metastable β-phase at 200°C produced changes in the resistance behavior of alloys which were found to be stable with respect to ω-phase precipitation at temperatures up to 400°C.

(9) Stabilization of the metastable β-phase produced an increase in the resistance of the alloys above 15% vanadium, in contrast to the observed decrease in resistance of these alloys during ω-precipitation at 450°C.

DISCUSSION

From the results of this investigation, there appears to be no low temperature athermal β to ω transformation. Moreover, it is possible that there is no direct martensitic transformation on quenching as suggested by Bagaryatskii. This is a result of the observation that the ω-phase forms by a thermally activated and apparently diffusion controlled process at increasingly rapid rates with decreasing vanadium content. This process proceeds at such a high rate that in the lower percentage composition alloys, it may not be able to be suppressed even by very rapid quenching.

It is not definite that the mechanism of ω-formation involves diffusion. It may be that the actual transformation from β to ω is a martensitic shear process, occurring at a specific composition which must first be attained by diffusion. However, it is certainly not normal bulk diffusion. As mentioned previously, this observation has also been made for Ti-V alloys by Krisement[13].

Probably the biggest conflict with an assumed diffusion mechanism is the lack of any change in the β-lattice parameter until long after the ω-precipitation has ceased. One possible explanation of this observation for a diffusion process lies in the very small size observed for the ω-precipitate.

In the Al-Cu system, Guinier[15] has advanced a theory to explain the lack of any change in the lattice parameter of these supersaturated alloys during the formation of copper-rich Guinier-Preston zones. In these alloys, it is known that the parent matrix is being depleted of copper by the formation of the zones. Guinier proposed that the G.P.

zones, even though they deplete the parent matrix, are so small (less than 100Å) and finely distributed throughout the matrix that they exert roughly the same dilatation effect on the parent matrix as the originally randomly distributed solute copper atoms. Thus, the zones themselves prevent the lattice parameters of the parent matrix from changing due to their own dilatation effect.

The results of the present work indicated that even when as much as 50 volume-% ω-phase is present, the minimum size of the ω-precipitates is 200-400Å in diameter. Thus, there must be very many of these small precipitates distributed throughout the β-matrix, which may well have the same dilatation effect as the originally randomly distributed solutes. It is interesting to note that when the β-peaks do begin to shift, the ω-peaks show a simultaneous increase in sharpness. This increase in sharpness may be attributed to a coalescing or loss of coherency of the small ω-precipitates which could relax their dilatation effect on the β-matrix.

Perhaps the best evidence for a diffusion controlled mechanism governing the formation of the ω-phase is the $t_a^{\frac{1}{2}}$ dependence observed for the formation of the ω-phase. This is the characteristic behavior of a precipitation process controlled by line diffusion[16]. In addition the increase in the ω-phase lattice parameter may also be associated with an increase in the titanium content of the ω-precipitate, which would require diffusion.

From the transition nature of the ω-phase, it seems reasonable that this phase would be poor in vanadium composition since, as can be seen in Figure 1, the α-phase has less than 2% solubility for vanadium at

room temperature. Such a loss of vanadium by the ω-phase as it is formed would mean increasing the vanadium content of the remaining β-phase, however, and would imply that there would be less tendency for the ω-phase to form in the higher composition alloys which are initially high in vanadium composition. This conclusion is in agreement with the observations of this investigation. Indeed, the rate of formation of the ω-phase decreases drastically with increasing vanadium content for one fixed temperature.

The combined indications of the diffusion process governing the ω-precipitation plus the small size and fine distribution of the precipitates provide the foundation for an interesting conjecture about the nature of the nucleation sites of the ω-precipitates.

It may be that in these metastable Ti-V alloys, there exist many, many small, very coherent embryos - or to be more specific, zones - which serve as nucleation sites for the ω-precipitation. In fact, as will be shown, the results of this investigation can be explained quite nicely by the assumption of the existence of these zones as very small regions of local distortion in the lattice. Many of the results obtained are in good agreement with results obtained by investigators working with materials known to contain zones.

It is a well known fact now that these zones are formed in aluminum-base alloys by a diffusion-controlled process at rates far in excess of those dictated by bulk diffusion[15]. The formation of these zones constitutes a pre-precipitation process, since no evidence of any new precipitate can be found by ordinary x-ray techniques. Only through the use of strictly monochromatic x-rays and single crystals can the

diffuse spots and streaks associated with these zones be observed. From such measurements, the size of these zones in Al-Cu alloys has been estimated at less than 100Å with over 50% of the copper concentrated in the zones after 48 hours at 25°C[17].

Perhaps the most interesting connection between the formation of these zones and the ω-precipitation is the time dependence of the process. Fine and Chiou, in studying zone formation in Al-4.2%Cu, have observed that the formation of these zones is proportional to $t_a^{\frac{1}{2}}$, where t_a = the annealing time[18]. As previously mentioned, this is the time dependence observed for the ω-precipitation process. Thus, it may be that the mechanism responsible for the ω-precipitation in Ti-V alloys is closely related to the mechanism of zone formation in the age hardening process in Al-Cu alloys.

The existence of a pre-precipitation process in the decomposition of these metastable Ti-V alloys has even been proposed by other investigators prior to this work. Knorr and Scholl, in investigating the internal friction behavior of quenched Ti-V alloys[19], deduced that below 280°C there was a definite pre-precipitation process prior to subsequent ω-precipitation.

Another interesting observation of the kinetics of zone formation has been made by Turnbull et al. in Al-2%Cu[20]. Turnbull observed that if the alloy was quenched to 0°C and then given a 2 min. reversion treatment at 200°C, the rate of zone formation after again quenching to 0°C was 2400 times slower than it was directly after the initial quench. This bears a striking resemblance to the effect of stabilization on the quenched Ti-V alloys as previously discussed. Thus,

again there is a strong indication of a relationship between the mechanism of zone formation and ω-precipitation in Ti-V alloys.

So far, however, there has been no direct evidence presented for the existence of zones in these quenched Ti-V alloys. It is believed that such evidence is presented in the results obtained for the effect of low temperature stabilization on the resistance of these quenched Ti-V alloys. As mentioned previously, the resistance of these alloys increases with stabilization time at 200°C, in contrast with the observed decrease in resistance during ω-precipitation, at 450°C (Figures 18 and 19).

Turnbull[20] and Panseri and Federighi[21] have observed similar effects during the formation of zones in Al-Cu and Al-Zn alloys. The results of Turnbull on the resistance of Al-Cu alloys during zone formation[20] are identical in almost every respect with those in Figure 18 for Ti-V alloys.

It should be noted that both Turnbull and Panseri and Federighi concluded that the nature and rate of the zone formation kinetics in these aluminum-base alloys involved quenched-in vacancies. Whether this is true for the present Ti-V alloys is uncertain, however, since nothing is known about the vacancy concentrations in the quenched alloys or the mobility of quenched vacancies in these alloys.

The one observation yet to be explained is the resistance behavior of these alloys at temperatures below 0°C. Here, several explanations are possible in terms of a zone structure.

The first possibility is that more zones (e.i.- small regions of local distortion) are formed by a diffusionless process as the temperature decreases. These new zones then increase the number of electron

scattering sites in the alloy, thereby increasing the resistance of the alloy. However, if this were the case, one might expect that the behavior of all the alloys would be the same except for a temperature scale factor. That is to say, a change in alloy composition would affect only the magnitude of the temperature dependence and not the functional form of the dependence.

Both Turnbull[20] and Panseri and Federighi[21] found that for a constant composition, all of the resistance vs. annealing time curves for aluminum-base alloys could be made to fit the same curve simply by adjusting the scale of the annealing time axis for each individual annealing temperature. Moreover, Turnbull[20] found that over the composition range 1.4%Ag to 8.5%Ag in Al-Ag alloys, there was very little change in the annealing time dependence of the zone formation in this alloy.

A second possibility for explaining the low temperature behavior of these quenched Ti-V alloys is an elastic dilatation of the matrix by the zones as the temperature decreases. This dilatation could increase the effective size of the electron scattering sites in the matrix and thereby raise the resistance of the alloy.

As has been stated before, there is reasonable evidence that the ω-phase is a vanadium poor phase. Thus, if the zones in these alloys are associated with the later precipitation of the ω-phase, it is likely that these zones are poor in vanadium, too. Thus, a decrease in temperature may thermodynamically supersaturate the zones. This supersaturation might then be relaxed by an associated thermoelastic dilatation of the zone and the surrounding matrix and thereby increasing the size of the electron scattering sites.

One last interesting point to note is the increasingly negative temperature coefficient of resistance with increasing vanadium content of the alloys. Based on the above argument, this would indicate a greater tendency for the zones to become supersaturated with decreasing temperature in the higher percentage alloys, which is not an unreasonable conclusion.

SUMMARY

In titanium-base alloys of 15% to 25% vanadium, the following summary gives the proposed mechanism for the precipitation of the ω-phase from the metastable β-phase:

(1) The ω-phase precipitates as very small particles at a very rapid rate which increases with decreasing vanadium content of the alloy. The process is apparently controlled by an enhanced diffusion mechanism which results in a titanium rich phase.

(2) There appears to be no direct low temperature martensitic transformation of β to ω. Moreover, the rapid rate of precipitation of diffusion formed ω-phase makes the possibility of such a transformation on quenching doubtful.

(3) There exists a pre-precipitation stage in these alloys which may well provide both the nucleation sites and the mechanism for later ω-phase precipitation.

(4) The small embryos or zones generated by this pre-precipitation process are responsible for the negative temperature coefficient of resistivity observed below $0^{\circ}C$ in these alloys.

(5) These zones are quite small and exhibit no definite crystalline structure different from that of the parent β-phase.

(6) These zones form at a very rapid rate and appear to be rich in titanium.

SUGGESTIONS FOR FURTHER WORK

Of primary importance is the actual detection of the zones in these metastable alloys. This will entail the use of strictly monochromatic x-rays and single crystals of the quenched alloys. The next step would be a study of these zones at low temperatures in order to determine the exact process affecting the resistance of the alloys.

A study of the dependence of the formation rate of the zones on the quenching rate and quenching temperature differential should be made in order to determine the nature of any quenched-in structural defects associated with the zone clustering.

Finally, a study of the effect of composition on the zone formation should be made in order to determine the effect of the metastable nature of the β-phase on quenched-in structural defects.

ACKNOWLEDGMENTS

The author wishes to acknowledge Dr. Franz R. Brotzen, Professor of Mechanical Engineering, for his guidance during the progress of this investigation.

The helpful discussions with Drs. J. M. Roberts, R. M. Asimow, and W. B. Pfeiffer are also gratefully acknowledged. Special thanks are extended to Dr. K. T. Aust for referring the author to the work of Turnbull and Rosenbaum.

The author is further indebted to the National Aeronautics and Space Administration for their sponsorship of this research. This research was sponsored under NASA contract number NsG-6-59.

APPENDIX I

The fundamental relationship describing the integrated intensity of a diffraction peak at angle 2θ as a function of the various angular and structural factors associated with it is given by:

(1) $S_x = \text{const. } A(\theta) \, [F(hkl)]^2 \, m \, P(\theta) \, e^{-M(\theta)} V_x / v_x^2$

where,

$A(\theta)$ = the angular adsorption factor

$F(hkl)$ = the structure factor of the peak

m = the multiplicity of the (hkl) plane

$P(\theta)$ = the Lorentz-polarization factor

$e^{-M(\theta)}$ = the temperature correction factor

v_x = the unit cell volume of the "x"-phase

V_x = the volume-% of the irradiated volume consisting of the "x"-phase

Since the indices of the diffraction peak being observed are known and the angular factors can be calculated, Equation (1) becomes,

$$S_x = K_x(hkl,\theta) \, A(\theta_x) \, V_x$$

where,

K_x = a calculated constant

Thus,

$$V_x = S_x / [K_x \cdot A(\theta_x)]$$

Similarly, for the "y"-phase we can find,

$$V_y = S_y / [K_y \cdot A(\theta_y)]$$

Thus,

$$V_x/V_y = (K_y/K_x) \cdot (S_x/S_y) \cdot [A(\theta_y)/A(\theta_x)]$$

$$= K(x,y) \cdot (S_x/S_y) \cdot [A(\theta_y)/A(\theta_x)]$$

$$= \gamma$$

where,

$K(x,y)$ = a calculated constant

For a two phase system, it is known that,

$$1 = V_x + V_y$$

or,

$$V_x = 1/(1 + V_y/V_x) = 1/(1 + \gamma)$$

$$V_y = (V_y/V_x)/(1 + V_y/V_x) = \gamma/(1 + \gamma)$$

BIBLIOGRAPHY

1. P. Duwez, Trans. ASM, 45 (1953), p. 934
2. P. Pietrokowsky and P. Duwez, Trans. AIME, 194 (1952), p. 627
3. F. R. Brotzen, E. L. Harmon, Jr., and A. R. Troiano, Trans. AIME, 203 (1955), p. 413
4. P. D. Frost, W. M. Parris, L. L. Hirsch, J. R. Doig, C. M. Schwartz, Trans. ASM, 46 (1952), p. 231
5. P. D. Frost, W. M. Parris, L. L. Hirsch, J. H. Doig, and C. M. Schwartz, Trans. ASM, 46 (1954), p. 1056
6. J. M. Silcock, M. H. Davies, and H. K. Hardy, The Mechanism of Phase Transformations in Metals, Inst. of Metals Monograph and Report Series No. 18 (1956), p. 93
7. Yu. A. Bagaryatskii, G. I. Nosova, and T. V. Tagunova, Dokl. Akad. Nauk SSSR, 105 (1955), p. 1225
8. Yu. A. Bagaryatskii and G. I. Nosova, Phys. of Metals and Metallography, 13 (1962), p. 92
9. J. M. Silcock, Acta Met., 6 (1958), p. 481
10. B. A. Hatt and J. A. Roberts, Acta Met., 8 (1960), p. 575
11. R. F. Hehemann, Proceedings of the USAEC Symposium on Zirconium Alloy Development, Cablewood, Pleasanton, California, Nov. 12-14, 1962, Vol. I, p. 10-0
12. M. Cohen and B. L. Averbach, Trans. AIME, 176 (1955), p. 401
13. O. Krisement, Z. f. Metallk., 45 (1960), p. 695
14. E. L. Harmon and A. R. Troiano, J. Metals, Fall Meeting Rpt., Coll. 57, 9(1957), p. 592
15. A. Guinier, J. Metals, 8 (1956), p. 673

16. C. Zener, J. Applied Phys., 20 (1949), p. 950

17. A. Guinier, Physica, 15 (1949), p. 148

18. M. E. Fine and C. Chiou, Trans. AIME, 212 (1958), p. 553

19. W. Knorr and H. Scholl, Z. f. Metallk., 51 (1960), p. 605

20. D. Turnbull, H. S. Rosenbaum, and H. N. Treaftis, Acta Met., 8 (1960), p. 277

21. C. Panseri and T. Federighi, Acta Met., 8 (1960), p. 217

22. H. B. Callen, Thermodynamics, J. Wiley, (1960), Ch. 13, p. 213

TABLES

TABLE I

COMPOSITION AND ANALYSIS OF Ti-V ALLOYS

Nominal Composition (At. wt.%)	V (%)	C (%)	N_2 (%)	O_2 (%)	H_2 ppm	Fe (%)
Ti-25%V	24.8	0.02	0.02	0.114	86	0.08
Ti-22.5%V	22.7	0.02	0.02	0.084	73	0.02
Ti-20%V	19.5	0.01	0.01	0.095	61	0.07
Ti-17.5%V	15.2	0.02	0.02	0.106	53	0.08
Ti-15%V	14.8	0.01	0.01	0.128	50	0.09

TABLE II

CALCULATED DIFFRACTION PEAKS FOR β- AND COHERENT ω-PHASES FOR Cu K_α RADIATION

2θ	ω	β
32.10°	0001	
39.56	$10\bar{1}1$	
39.56	$11\bar{2}0$*	110*
46.00	$20\bar{2}0$	
51.80	$11\bar{2}1$	
57.14	$20\bar{2}1$*	200*
67.24	0002	
71.84	$12\bar{3}1$	
71.84	$30\bar{3}0$*	211*
81.26	$11\bar{2}2$	
81.26	$30\bar{3}1$	
85.22	$22\bar{4}0$*	220*
93.94	$22\bar{4}1$	
98.00	$13\bar{4}1$	
98.34		310
111.96	0003*	222*
111.96	$40\bar{4}1$	

where,

a_β = 3.20 Å (Ti-20%V)

$c_\omega = \sqrt{3}/2\ a_\beta$, $a_\omega = \sqrt{2}\ a_\beta$

* Parallel, equivalent planes in the β- and ω-phases

TABLE III

CALCULATION OF VOLUME % ω-PHASE

VS. ANNEALING TIME FOR A Ti-20%V ALLOY

t_a*	$2\theta_\beta$	$2\theta_\omega$	S_β	S_ω	S_ω/S_β	γ	%β	%ω
0*	39.87°	---	726	---	---	---	100.0	---
20	39.87	39.76	602	378	0.628	0.437	69.6	30.4
40	39.87	30.64	421	381	0.905	0.630	61.3	38.7
60	39.88	39.58	313	341	1.089	0.758	56.9	43.1
80	39.88	39.52	246	509	2.069	1.440	41.0	59.0
100	39.88	39.48	228	541	2.373	1.652	37.7	62.3
120	39.88	39.45	211	524	2.483	1.728	36.6	63.4
140	39.89	39.43	205	580	2.829	1.969	33.7	66.3
180	39.89	39.34	132	640	4.848	3.374	22.9	77.1

Annealing temperature = 425 $\pm$ 5°C

K (ω,β) = 0.696

*t_a in seconds

FIGURES AND GRAPHS

TABLE OF ABBREVIATIONS

USED IN GRAPHS

T_a = annealing temperature

T_i = temperature of stabilization by incubation

t_a = time at annealing temperature

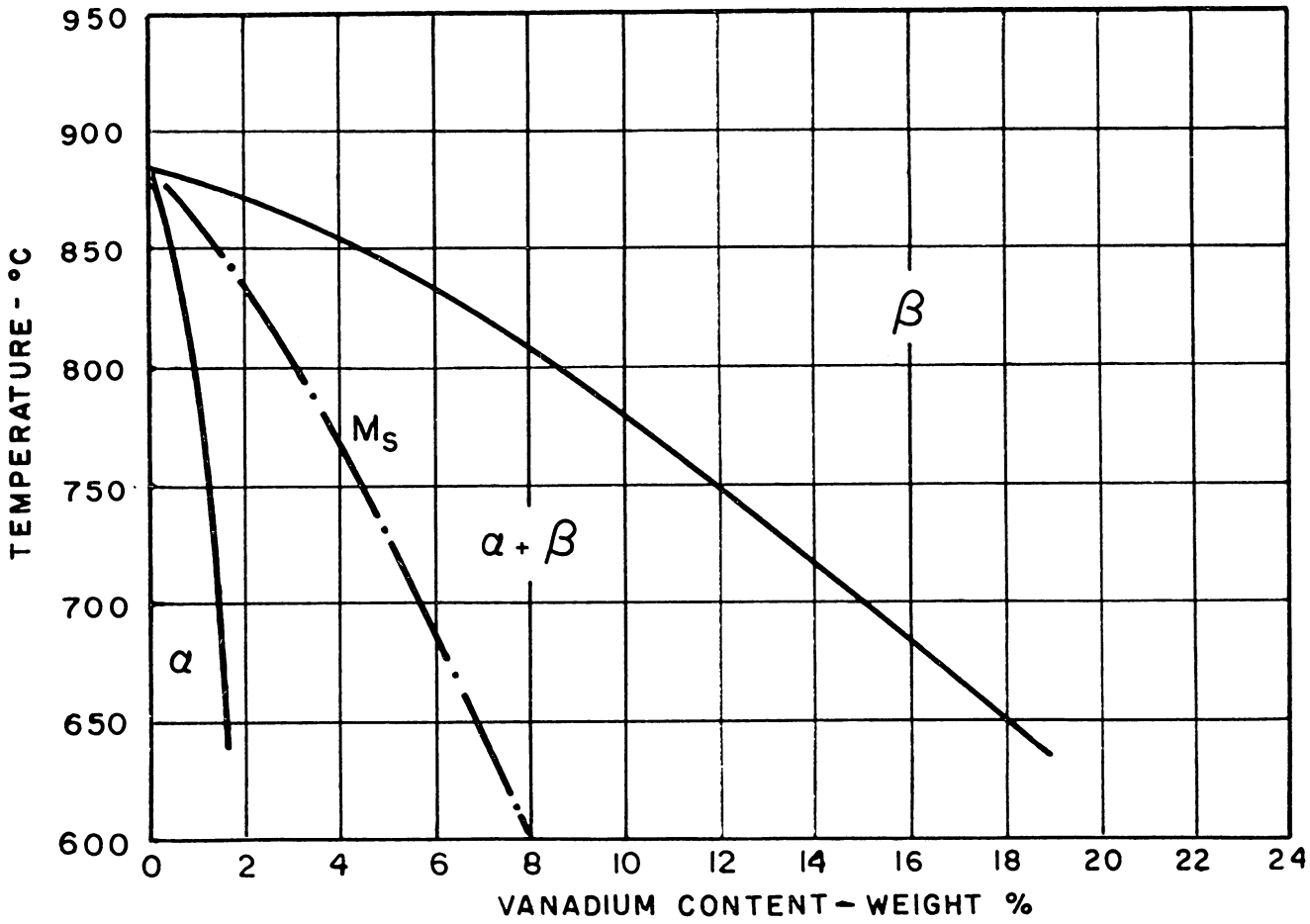

FIG. 1 - Partial Ti-V Phase Diagram, F(%V)

(from Pietrokowsky & Duwez - Ref. 2)

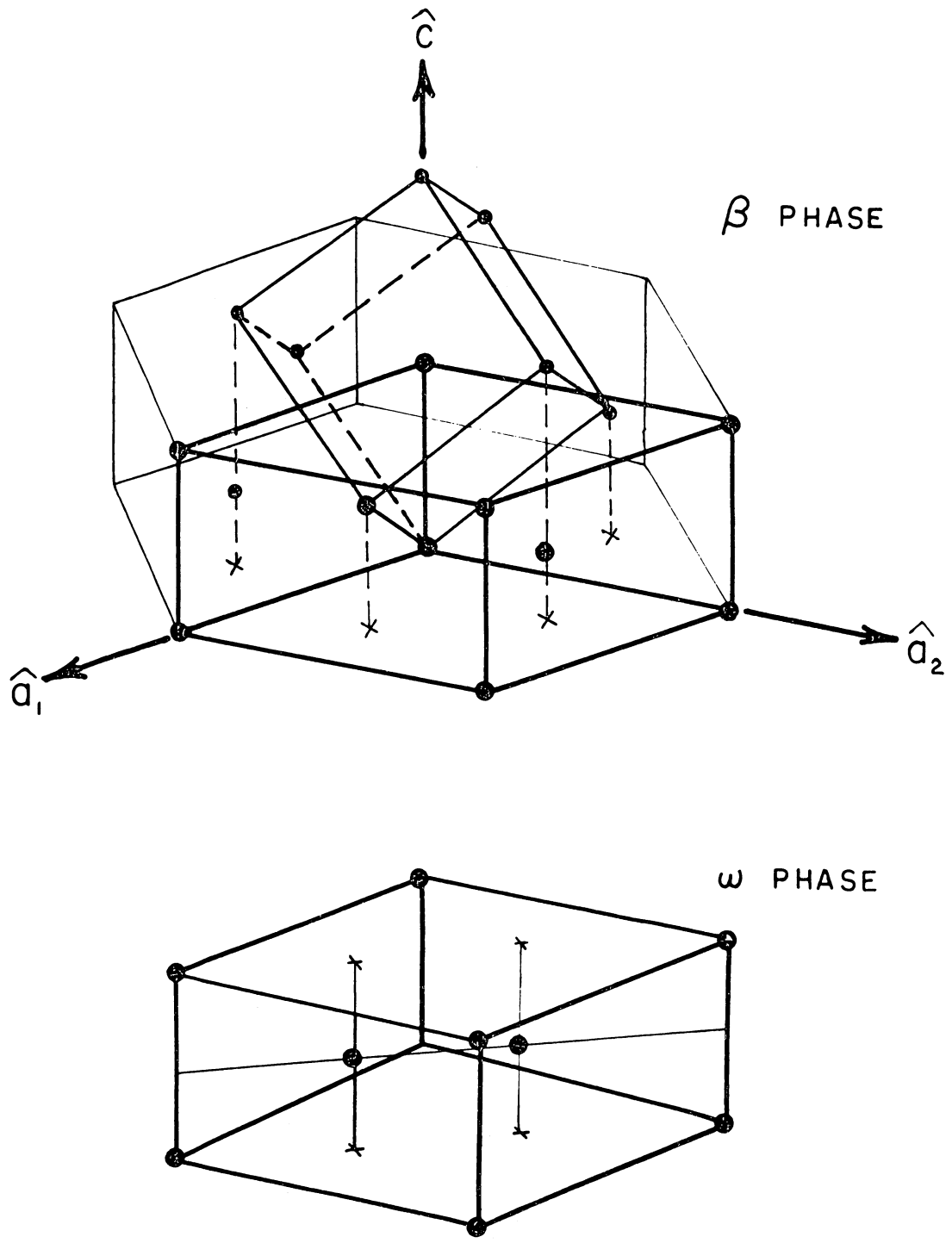

FIG. 2 - Structural Relationship of the ω and β Phases

(from Bagaryatskii & Nosova - Ref. 7)

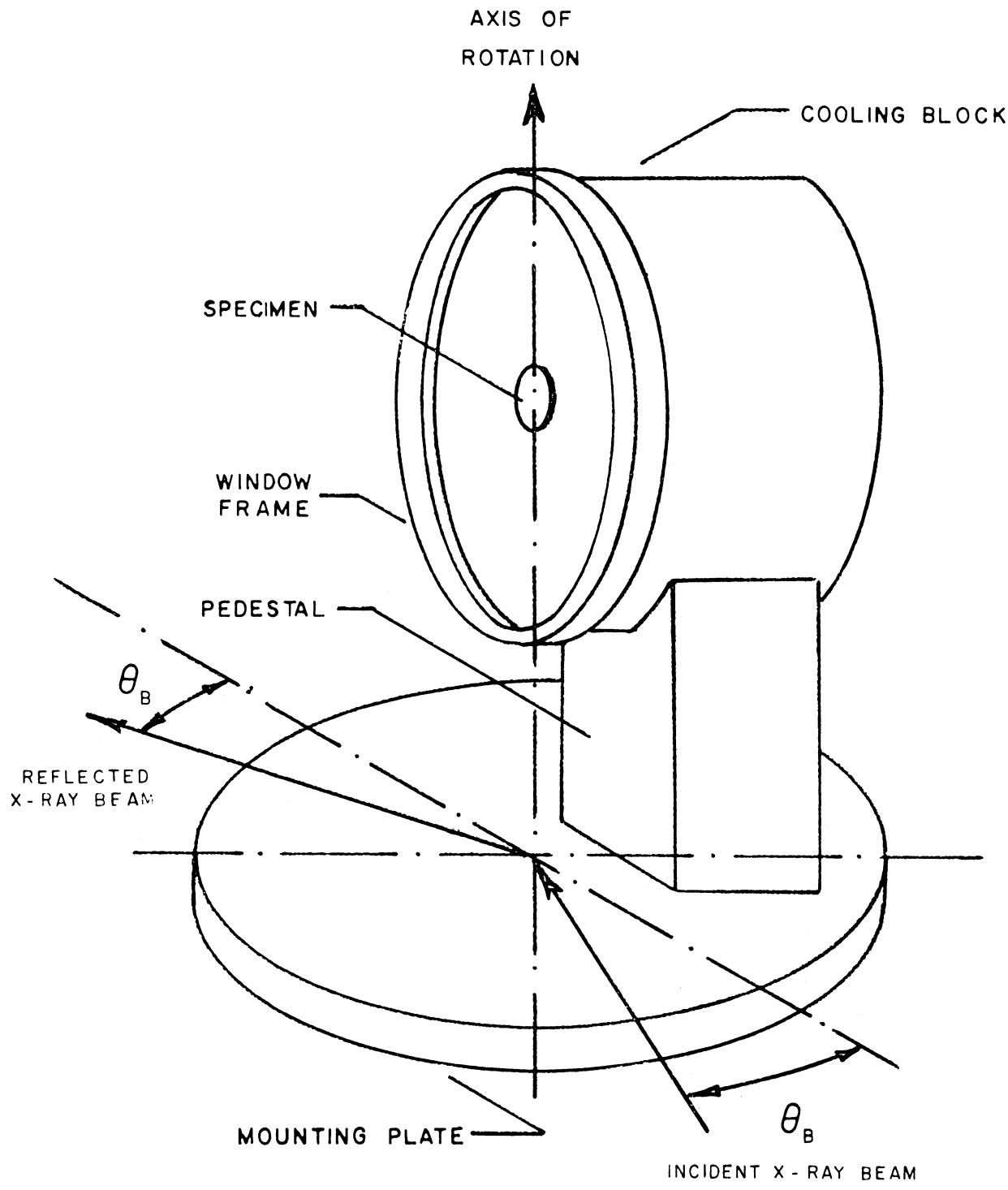

FIG. 3 - Low Temperature X-Ray Diffraction Specimen Mount

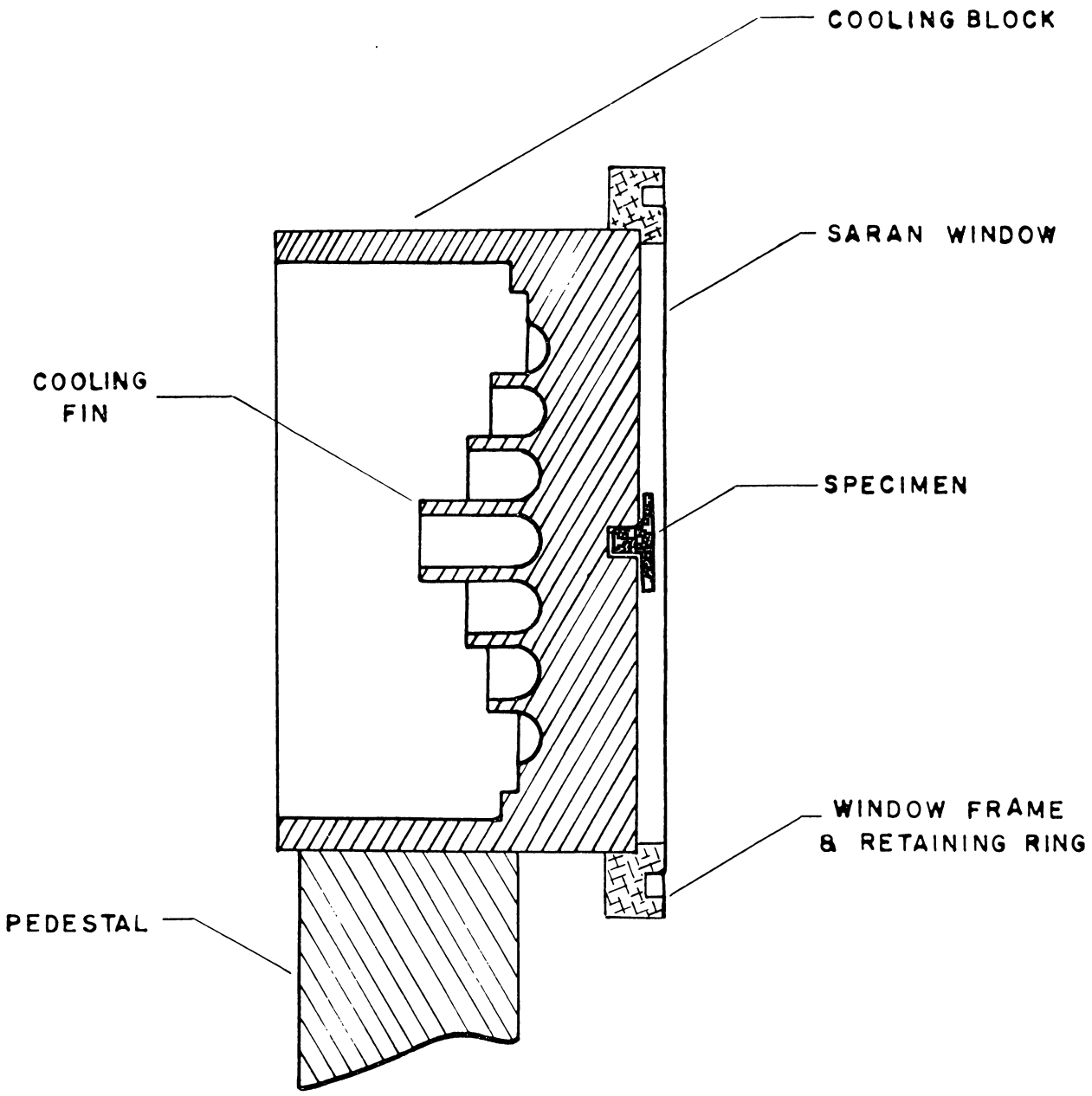

FIG. 4 - Cross-Section of Low Temperature X-Ray Mount

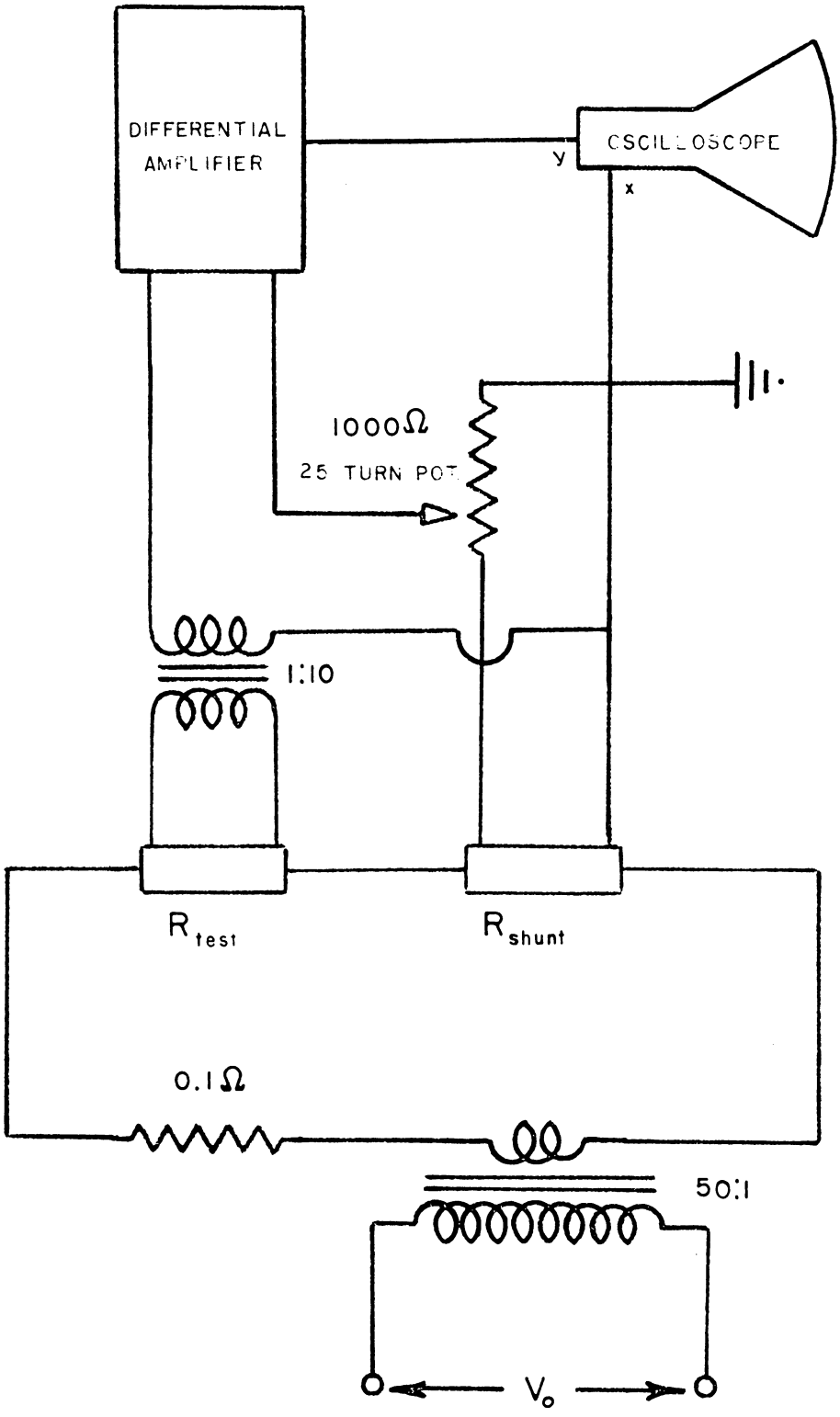

FIG. 5 - Resistance Measuring Circuit

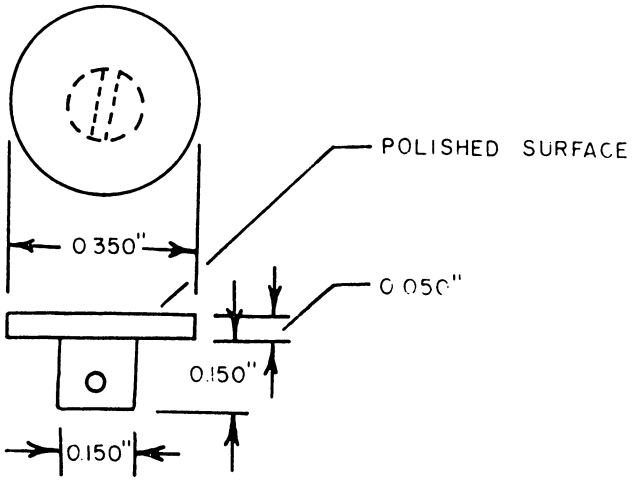

X-RAY SPECIMEN

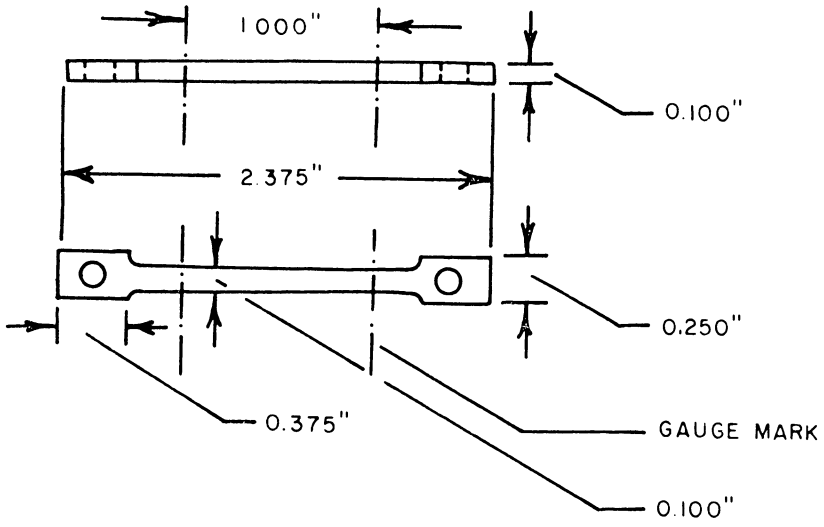

RESISTIVITY SPECIMEN

FIG. 6- RESISTIVITY & X-RAY SPECIMENS

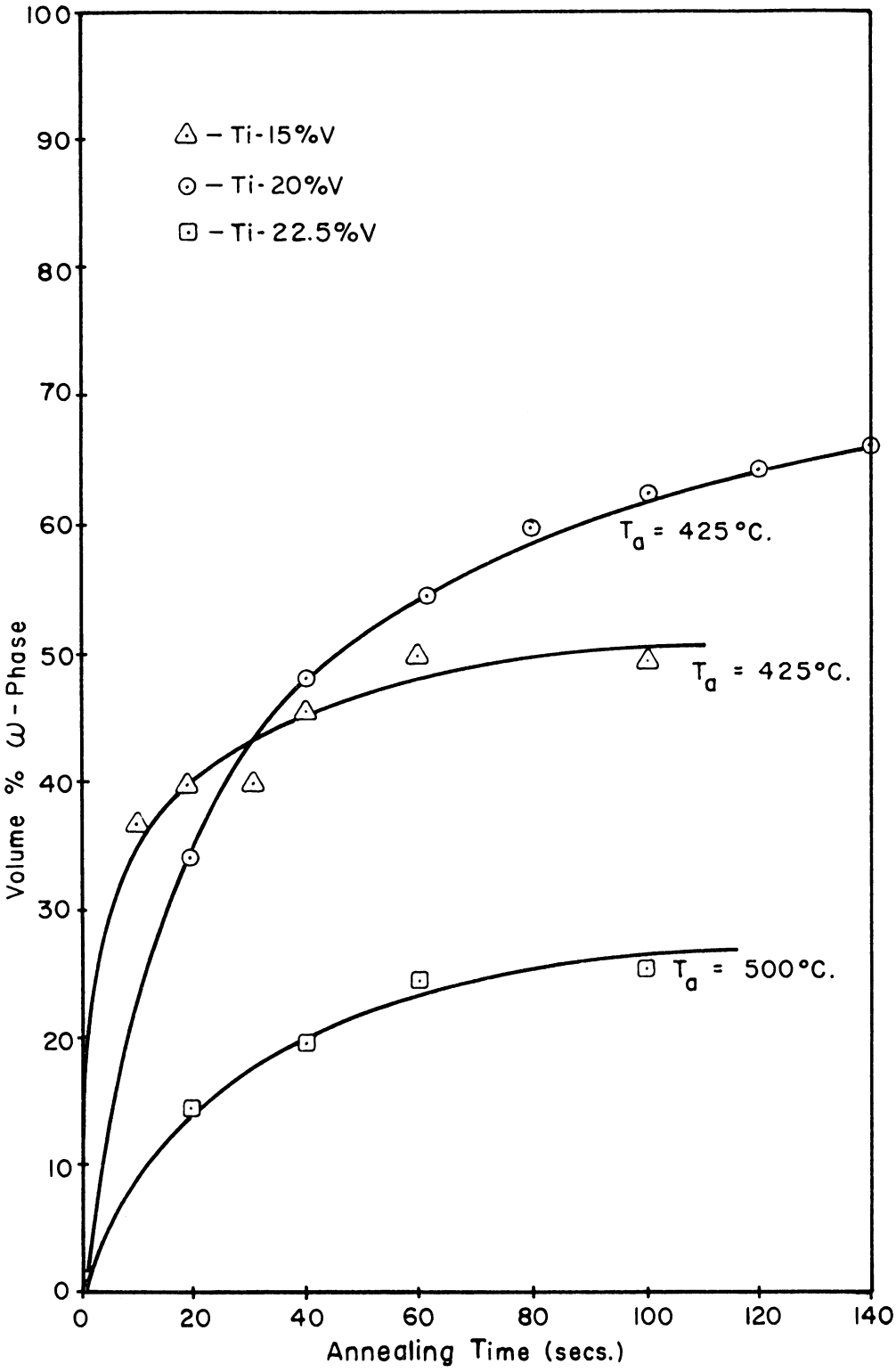

FIG 7 - Volume % ω-Phase vs. Annealing Time as a Function of % Vanadium.

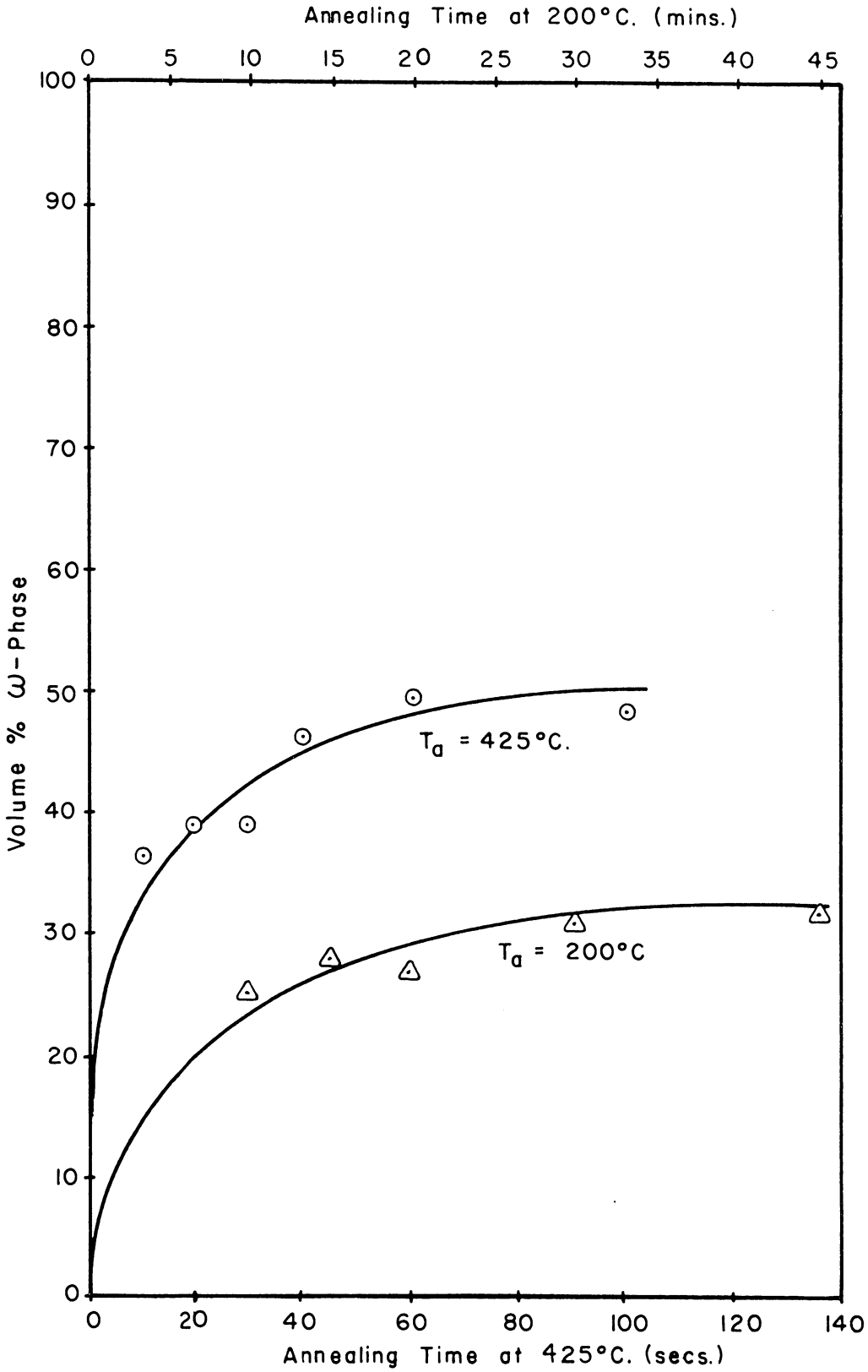

FIG. 8 - Volume % ω-Phase vs. Annealing Time in Ti-15%V

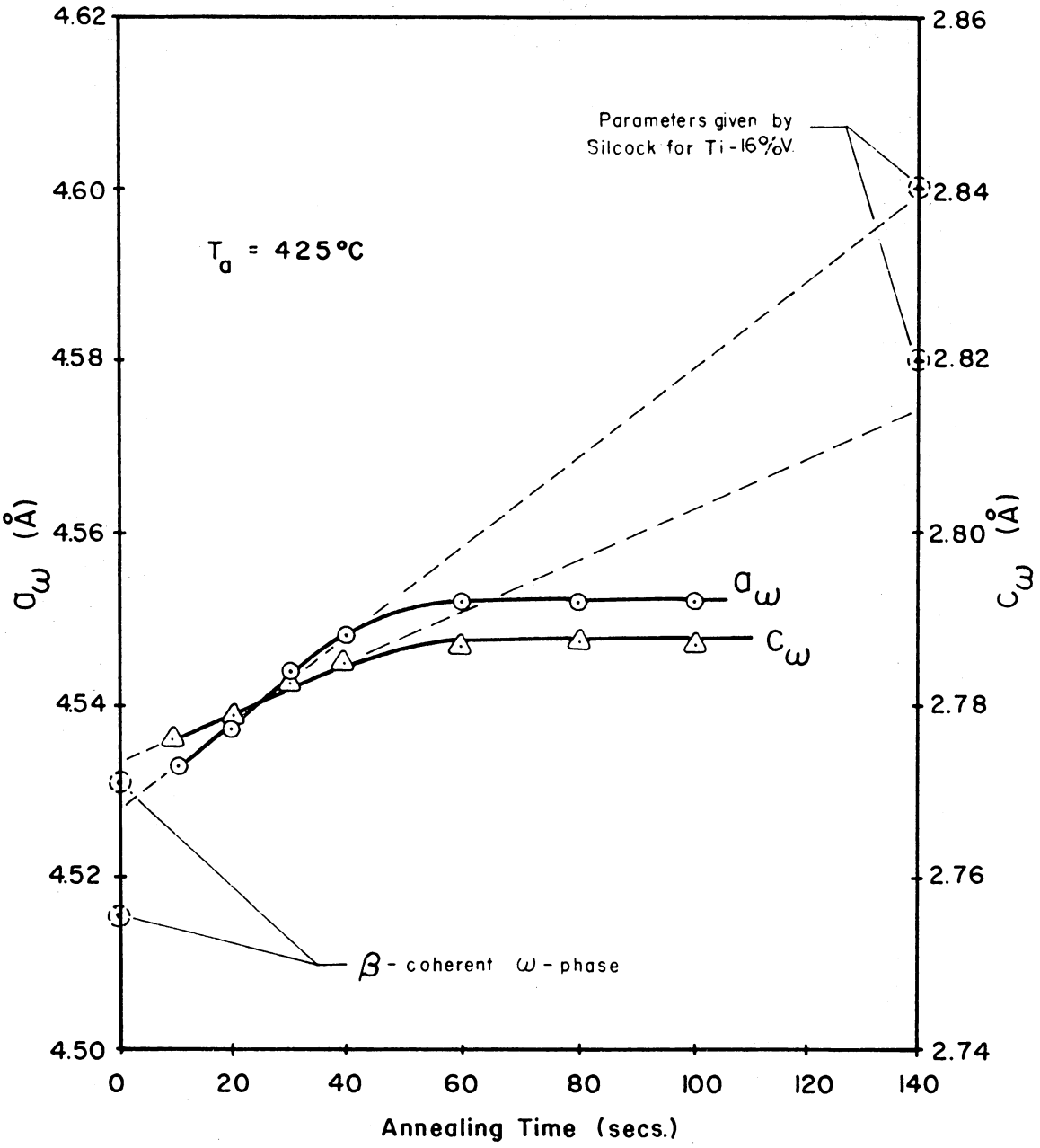

FIG. 9 - ω-Phase Lattice Parameters vs. Annealing Time in Ti-15%V.

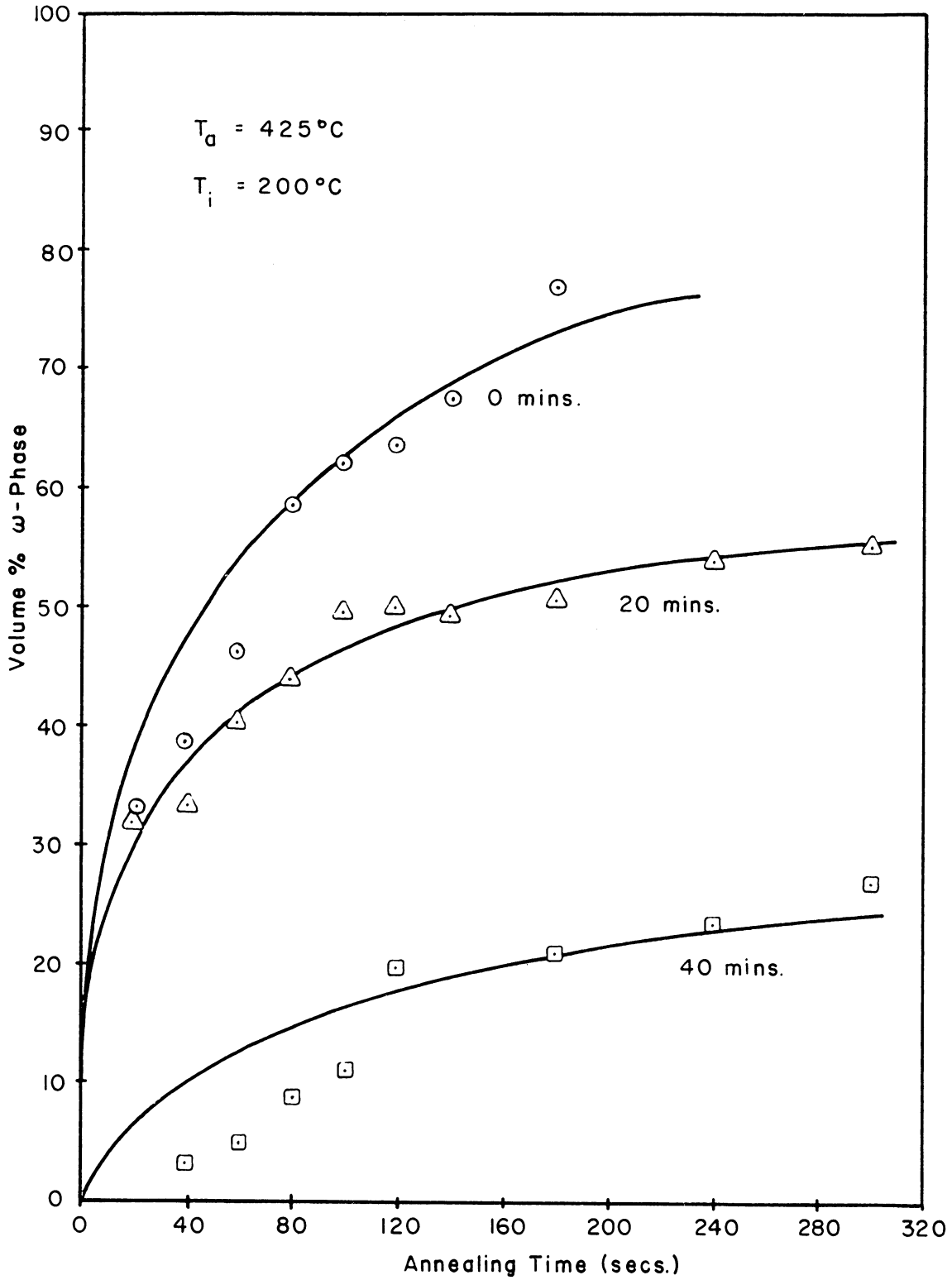

FIG. 10 - Volume % ω-Phase vs. Annealing Time in Ti-20%V as a Function of Incubation Time.

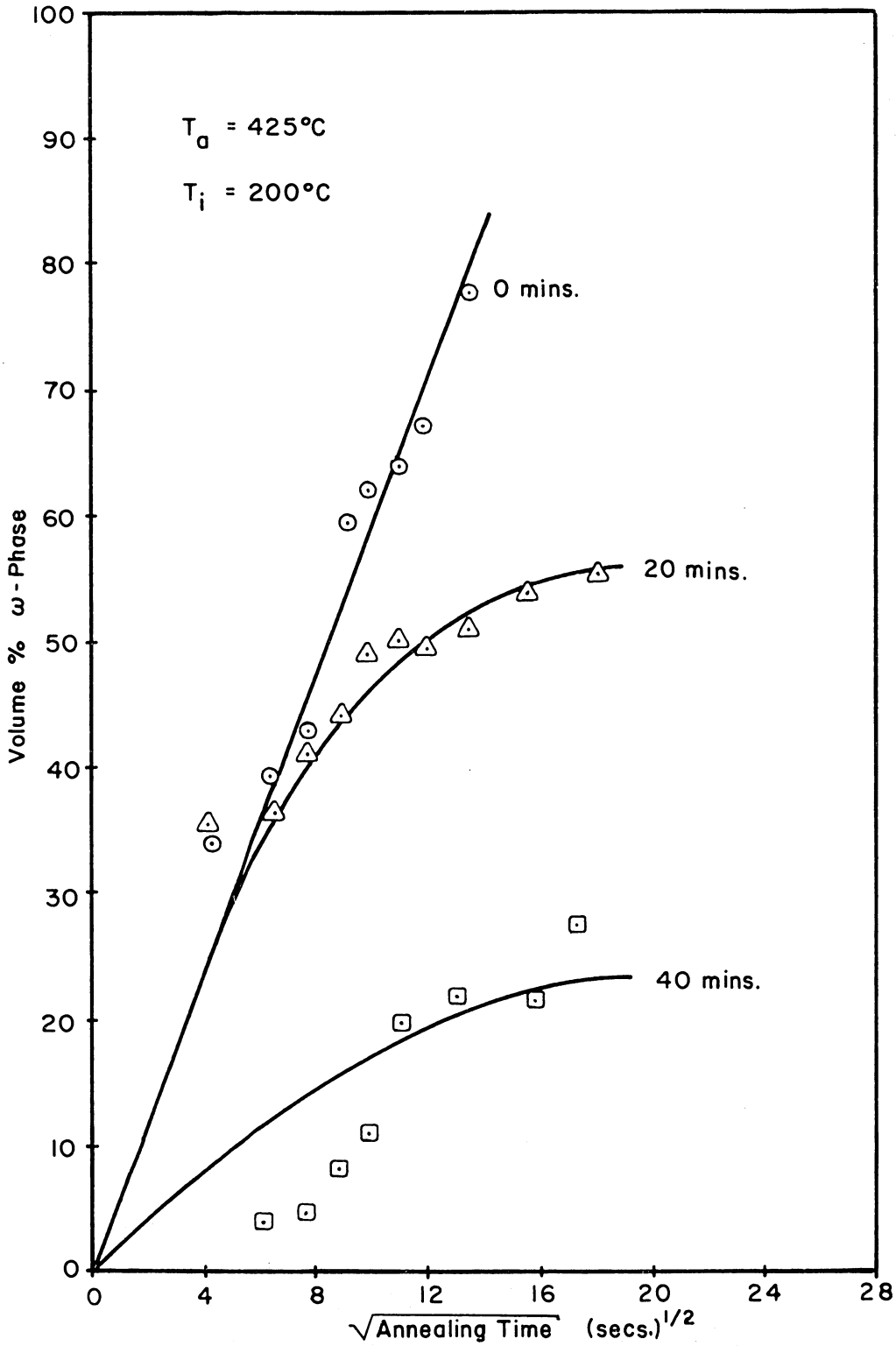

FIG. 11 - Volume % ω-Phase vs. (Annealing Time)$^{1/2}$ as a Function of Incubation Time in Ti - 20%V.

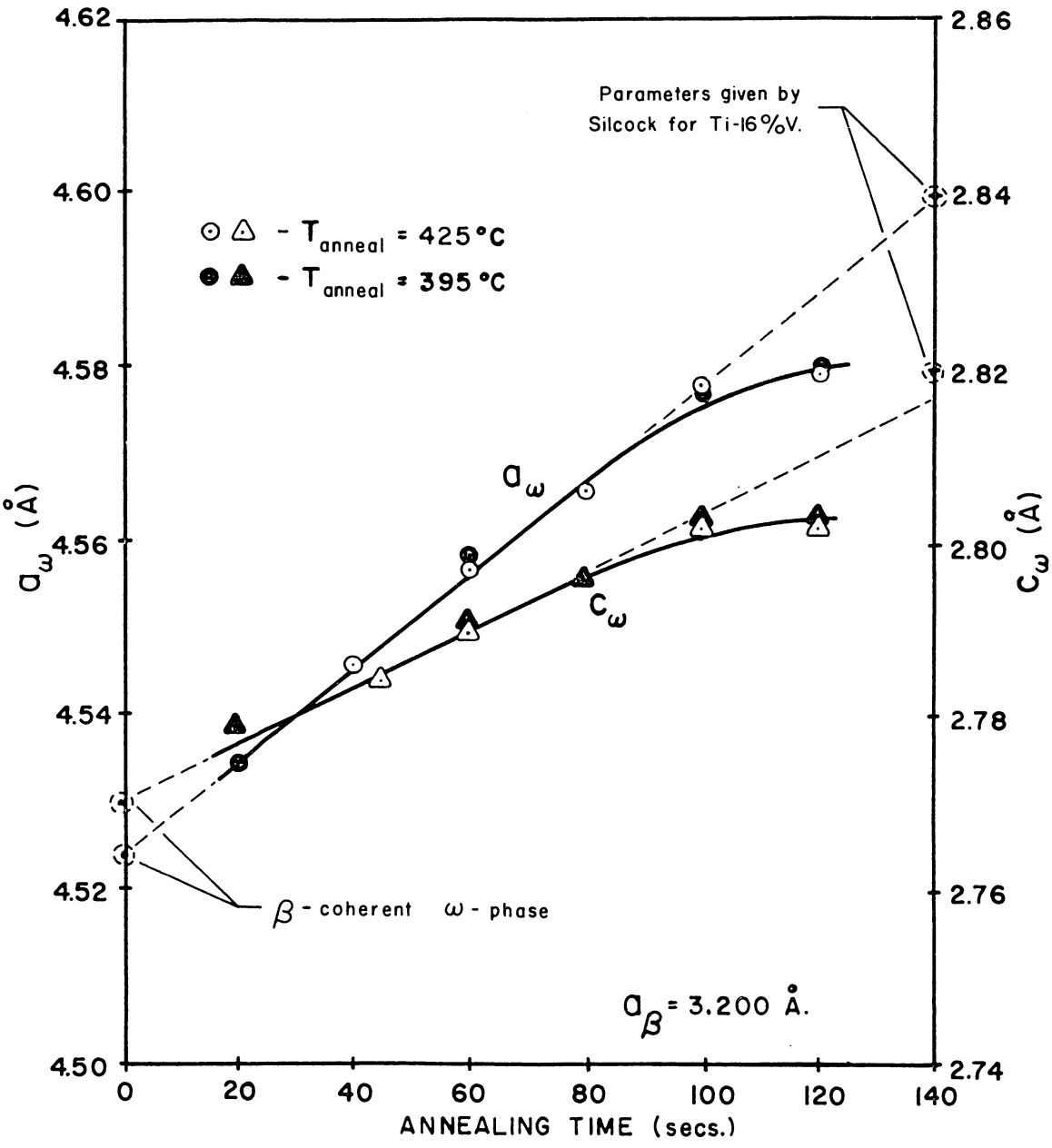

FIG. 12- LATTICE PARAMETERS OF THE ω-PHASE IN TI-20%V VS. ANNEALING TIME

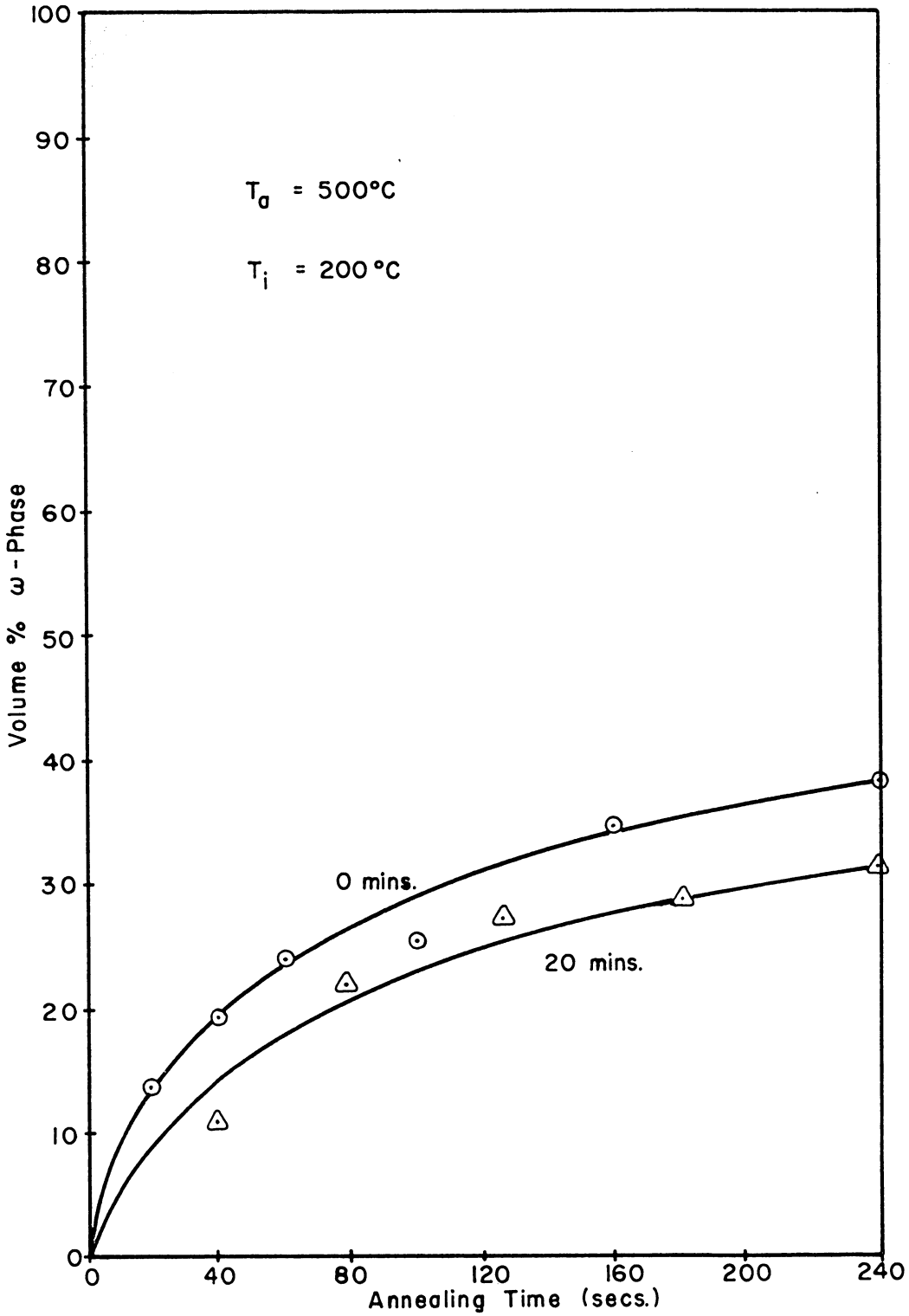

FIG. 13 - Volume % ω-Phase vs. Annealing Time in Ti-22.5%V as a Function of Incubation Time.

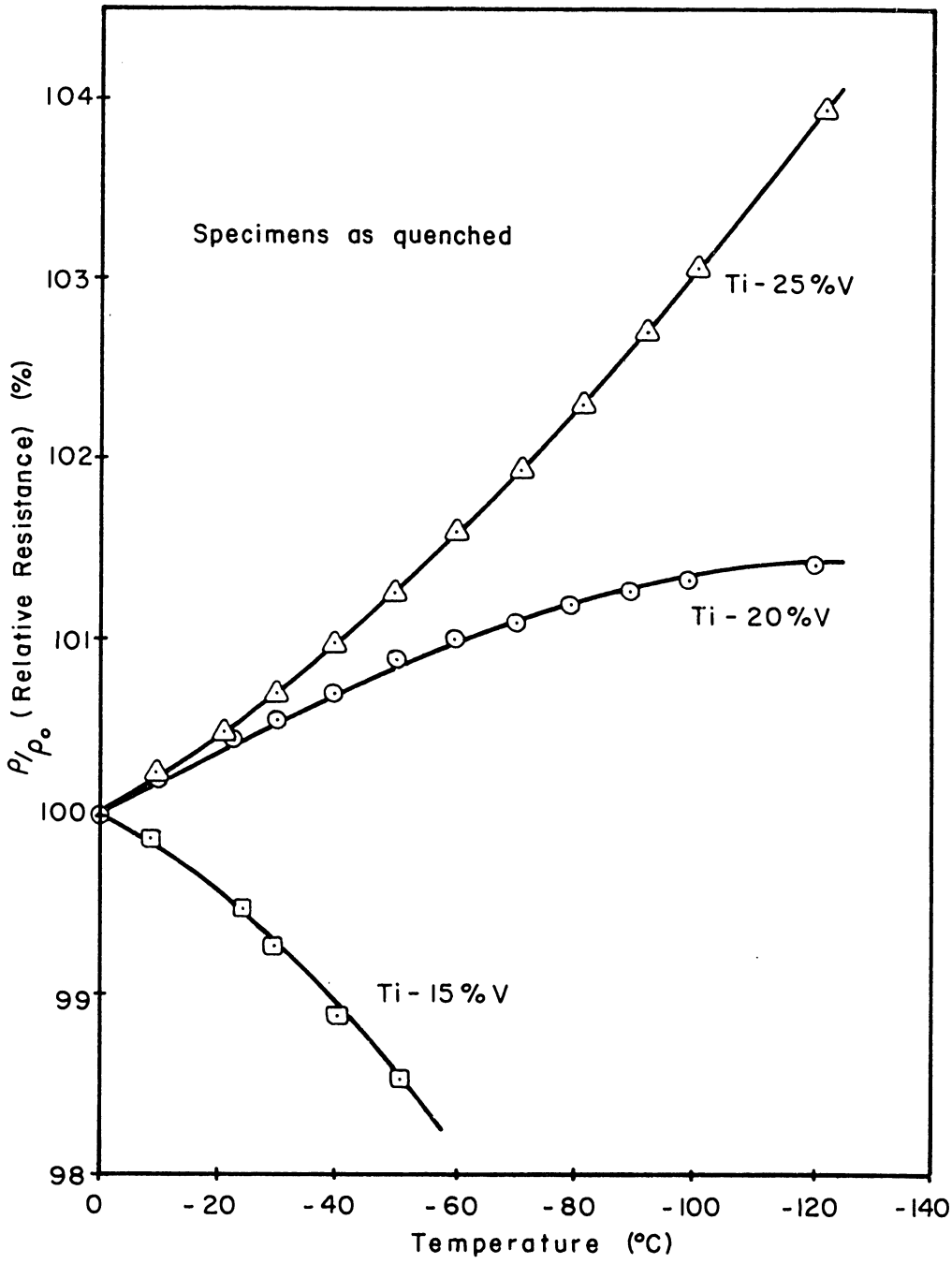

FIG. 14 - Relative Resistance vs. Temperature as a Function of % Vanadium.

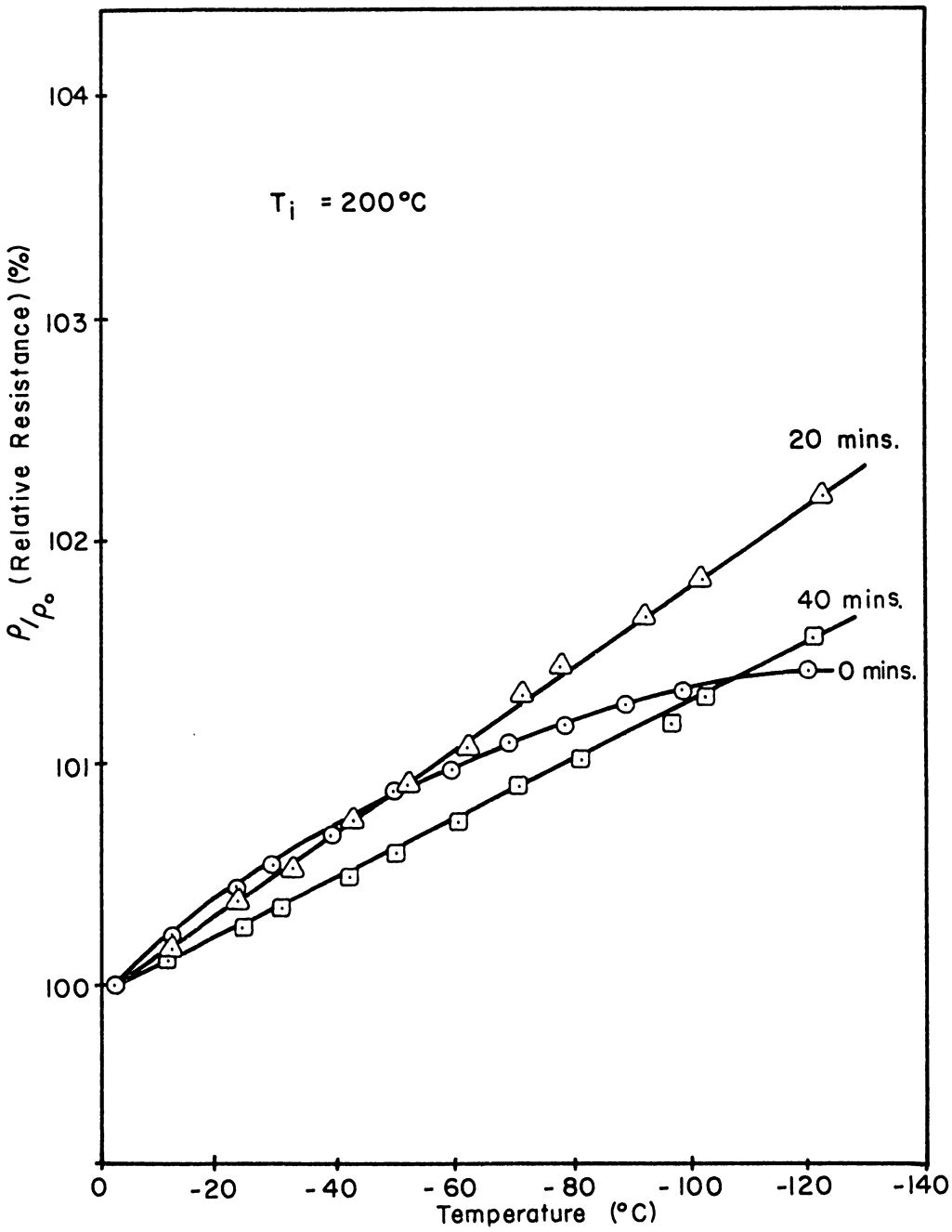

FIG. 15 - Relative Resistivity vs. Temperature in Ti-20%V as a Function of Incubation Time.

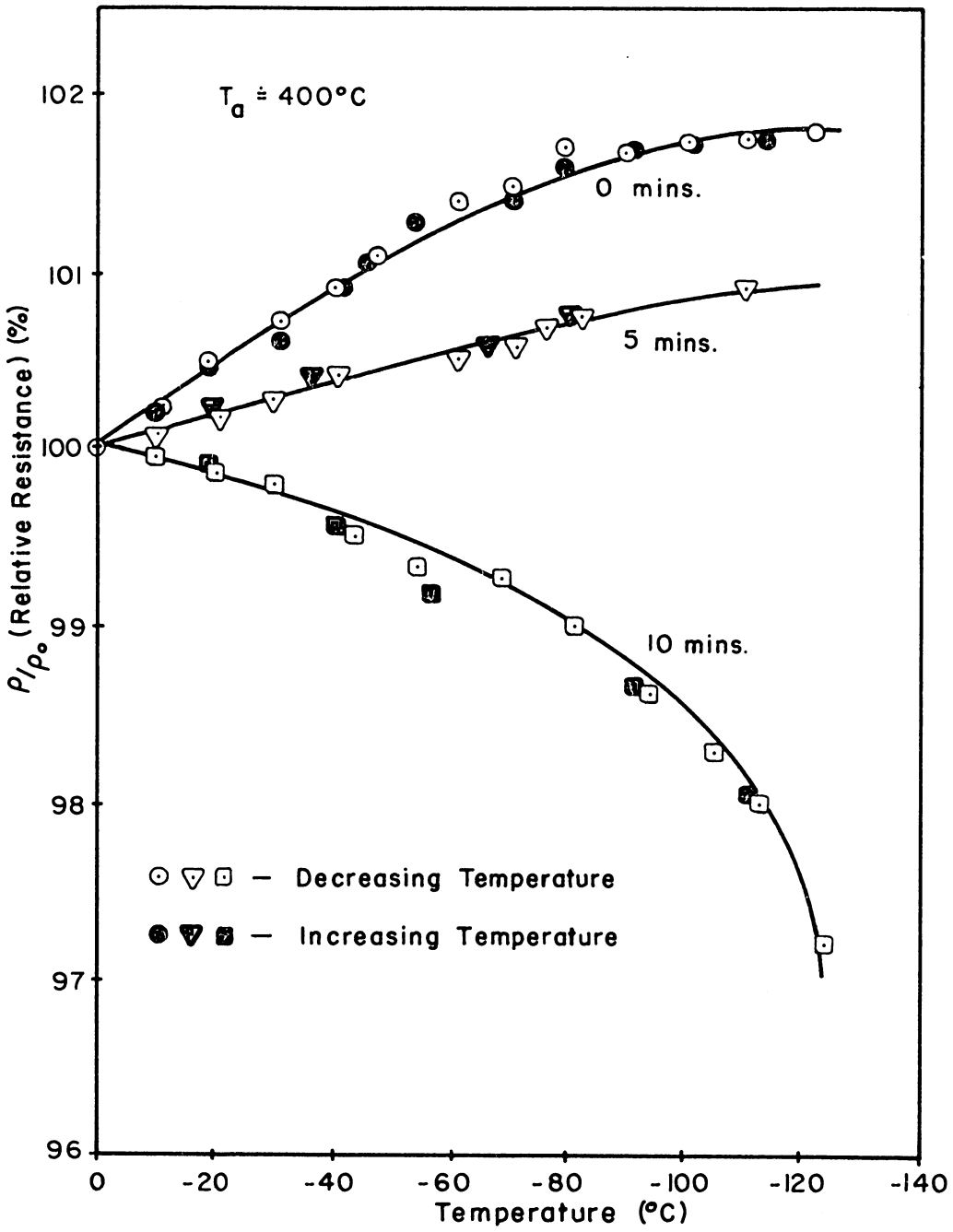

FIG. 16 - Relative Resistance vs. Temperature in Ti-20%V as a Function of Annealing Time.

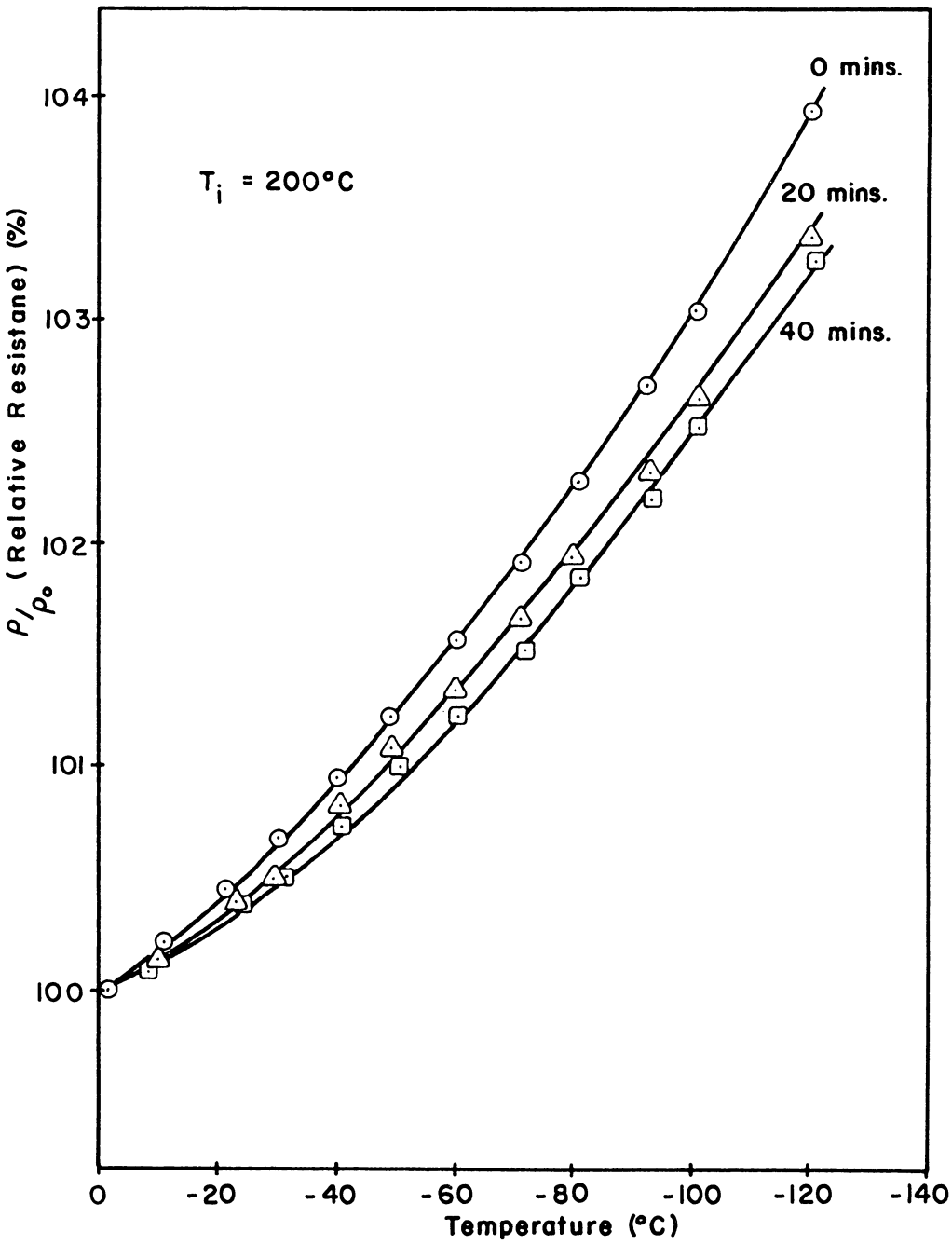

FIG. 17 - Relative Resistance vs. Temperature in Ti-25%V as a Function of Incubation Time.

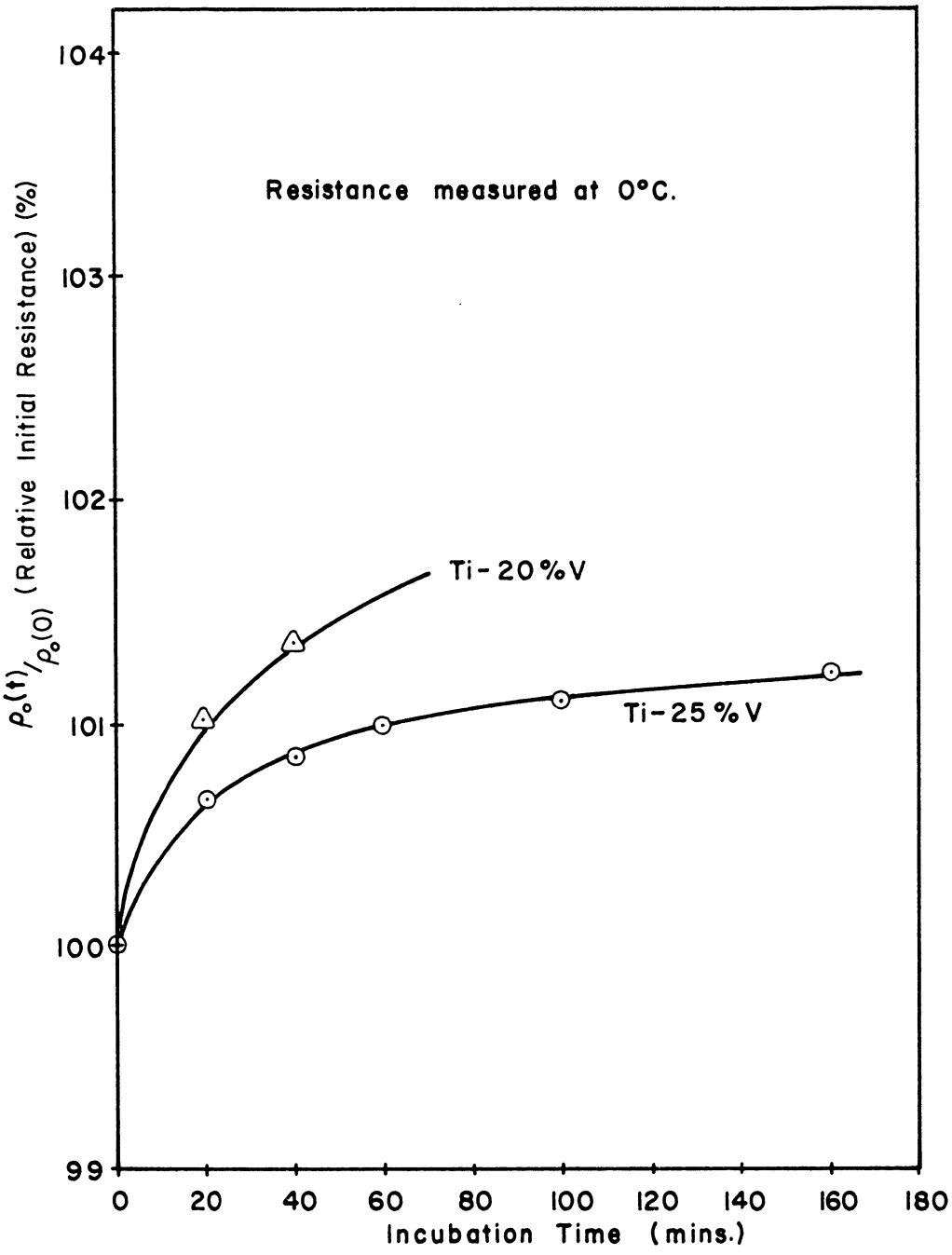

FIG. 18 - Relative Initial Resistance vs. Incubation Time as a Function of % Vanadium.

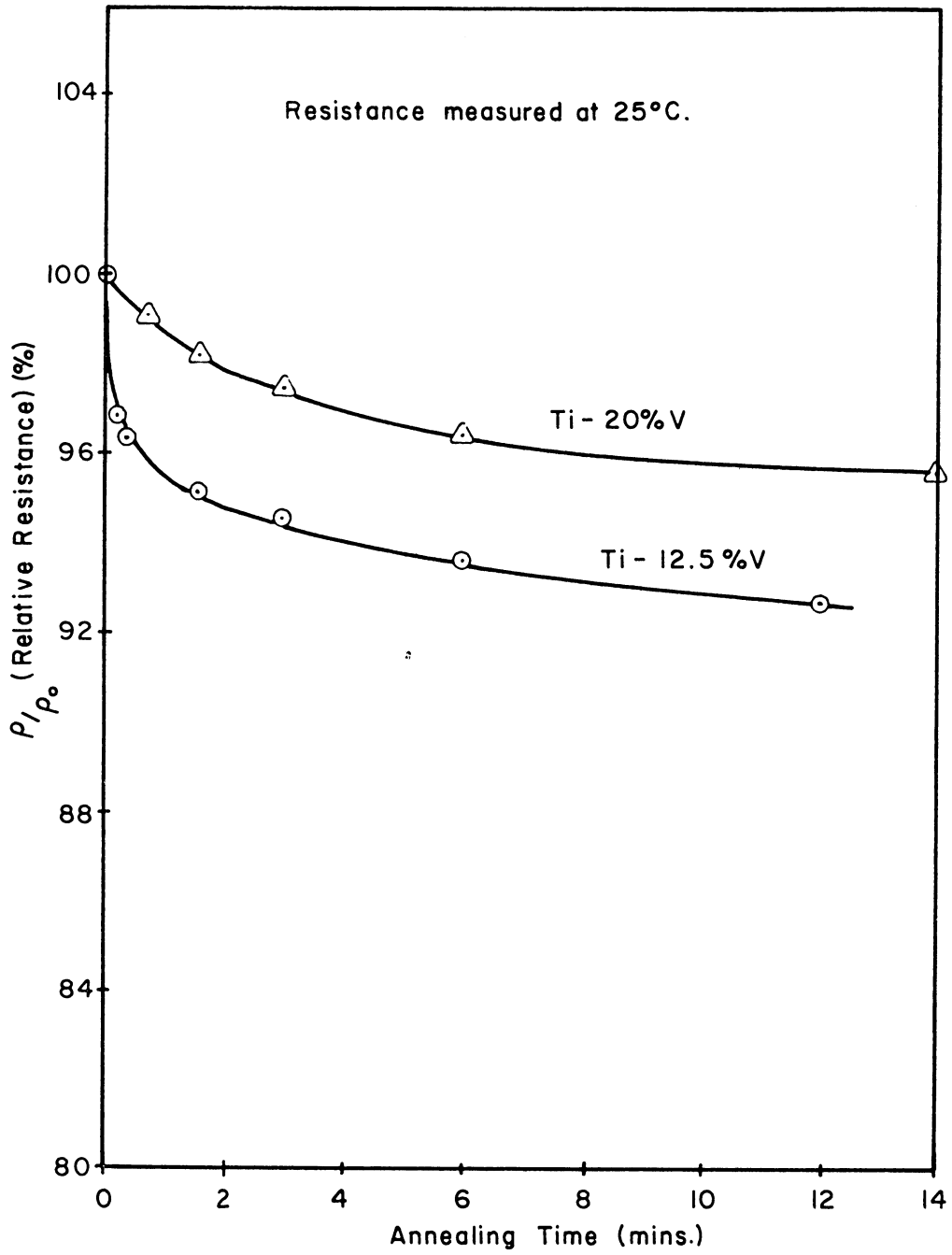

FIG. 19 - Relative Resistance vs. Annealing Time as a Function of % Vanadium.

(from Brotzen et. al. - Ref. 3)

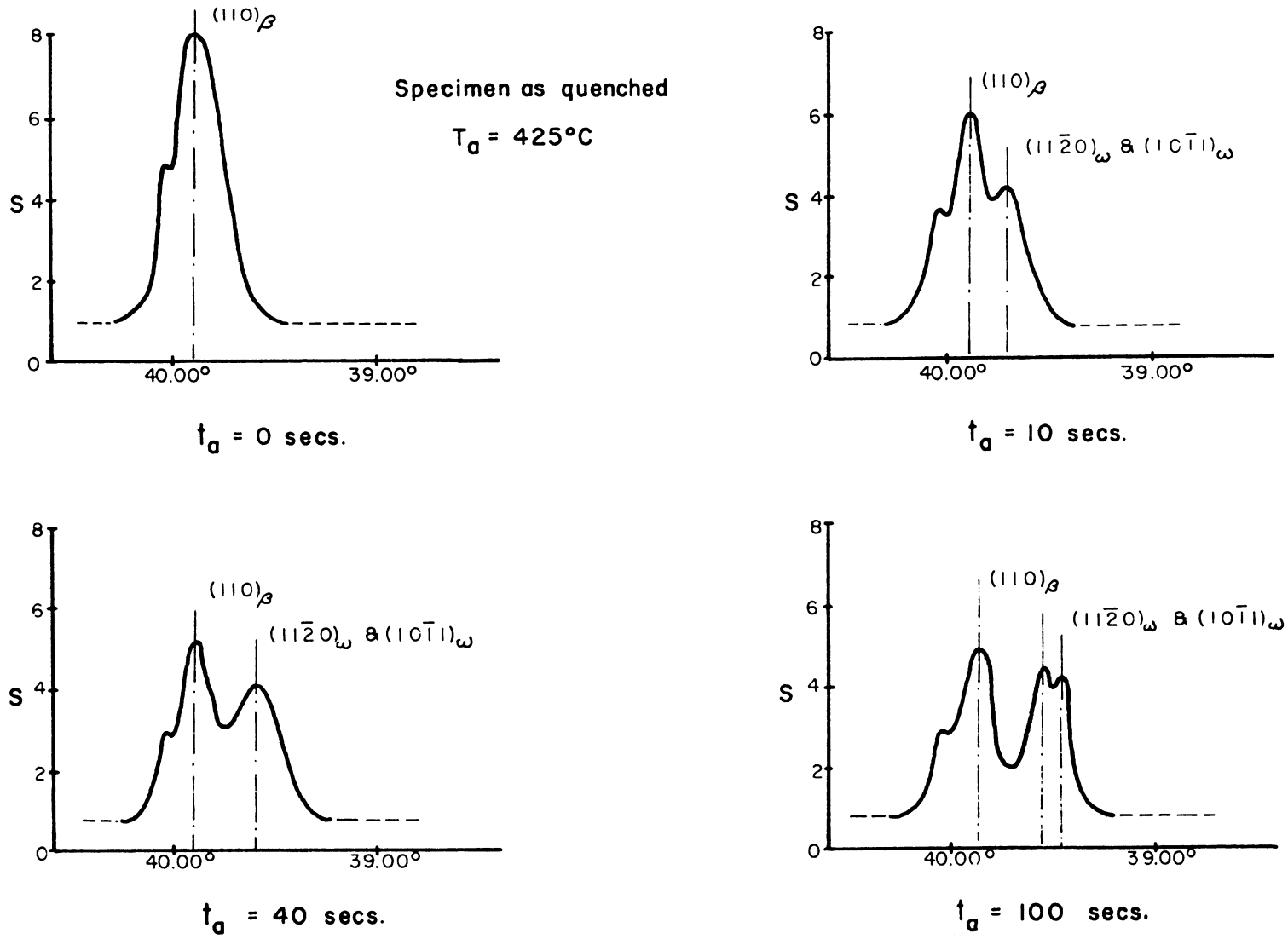

FIG. 20 - Diffraction Peaks of Ti-15%V as a Function of Annealing Time. (Cu K_α Radiation.)

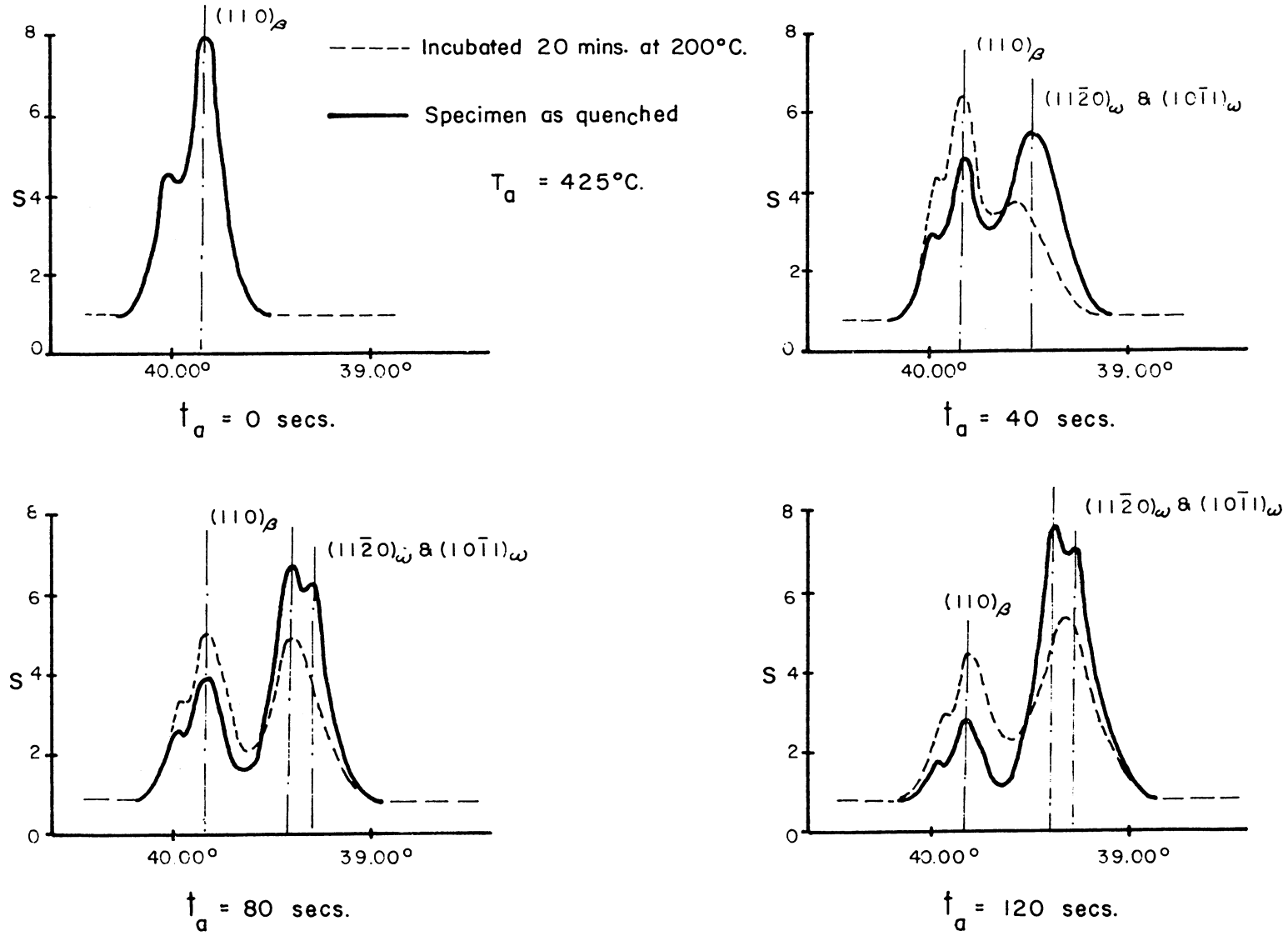

FIG. 21 – Diffraction Peaks of Ti-20%V as a Function of Annealing Time. (Cu K_α Radiation.)

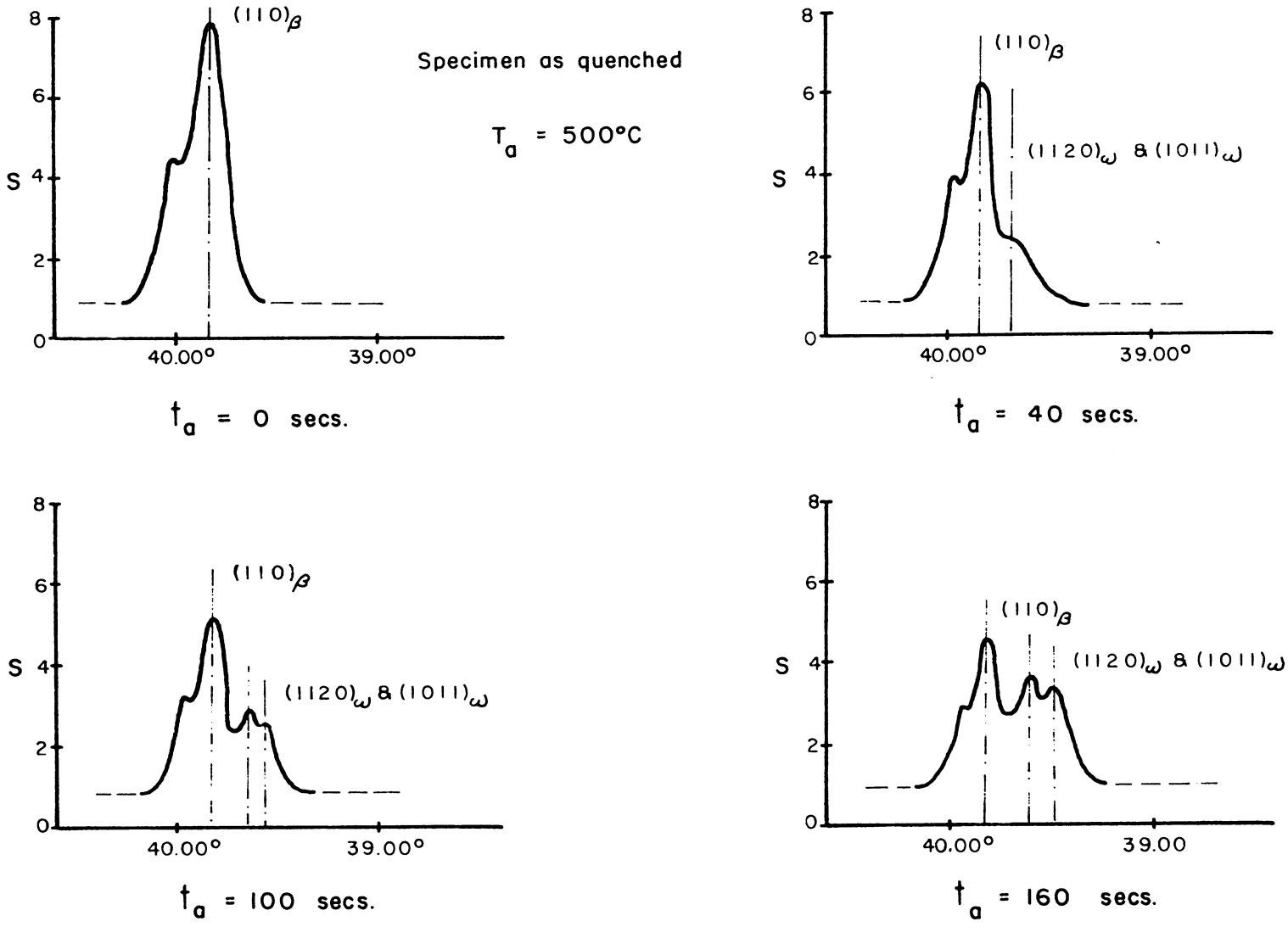

FIG. 22 – Diffraction Peaks of Ti-22.5%V as a Function of Annealing Time. (Cu K_α Radiation.)